Food and Bioprocess Technology
https://doi.org/10.1007/s11947-023-03112-2

RESEARCH

Optimization of the Radiofrequency Low-Pressure Cold Plasma Conditions for Decontamination of Saffrons

Mahsa Khodabandeh[1] · Majid Azizi[1] · Babak Shokri[2,3] · Masoumeh Bahreini[4] · Hasan Rezadoost[5] · Mohammad Salehi[2]

Received: 6 March 2023 / Accepted: 24 April 2023

Abstract

Cold plasma is an emerging non-thermal processing technology that could fulfill the food industry's need for decontamination purposes without compromising the quality if optimized in terms of plasma parameters, including feed gases, voltage, and exposure time. Different food matrices require specialized optimized processes due to the interactions between plasma and the food. In the present study, the response surface methodology was applied to optimize the radiofrequency low-pressure cold plasma processing of saffron (*Crocus sativus* L. stigmas.) with the aim of achieving the highest decontamination level with the least harm to metabolites. The effects of the treatment time, power, and three gas mixtures (X, Y, and Z) consisting of air, oxygen, and argon on 22 responses related to microbial load and quality of saffron were evaluated in 42 experiments. Eleven critical responses that determine the final quality of saffron were considered to calculate the desirable function as a comprehensive approach for optimization. Analyses showed that all factors significantly affected the desirable function, and the fitted linear model was significant. The optimal condition was determined as an RF power of 76 W for 26 min using the "*Y*" gas mixture, which reduced the total microorganisms, *coliforms*, *Escherichia coli*, molds, and yeast by 5.75, 6.71, 6.07, and 4.00 log CFU g^{-1} respectively. The optimal condition preserved saffron quality within category I of the ISO specification No. 3632-1. The experimental values were in accordance with the predicted values. Optical emission spectroscopy revealed that the main plasma reactive species were Ar^+ species, monoatomic oxygen, O^{2+}, O^+ ions, excited N_2 species, and N_2^+ ions. The temperature of the samples after treatment was in the range of 40–44 °C. Scanning electron microscopy of the saffron threads indicated surface etching. Our findings showed that saffron was disinfected without substantial harm to its appearance and metabolites by applying appropriate plasma treatment.

Keywords *Crocus sativus* L. · Decontamination · *Escherichia coli* · Optical emission spectroscopy · Optimization · RF plasma

✉ Majid Azizi
azizi@um.ac.ir

✉ Hasan Rezadoost
h_rezadoost@sbu.ac.ir

[1] Department of Horticultural Science and Landscape Architecture, Faculty of Agriculture, Ferdowsi University of Mashhad, Mashhad, Iran

[2] Laser and Plasma Research Institute, Shahid Beheshti University, G.C., Evin, Tehran 1983963113, Iran

[3] Department of Physics, Shahid Beheshti University, G.C., Evin, Tehran 1983963113, Iran

[4] Department of Biology, Faculty of Sciences, Ferdowsi University of Mashhad, Mashhad, Iran

[5] Department of Phytochemsitry, Medicinal Plants and Drugs Research Institute, Shahid Beheshti University, Evin, Tehran, Iran

Introduction

Aromatic spices were mostly treated like currency in the business world of the past because of their valuable, luxurious, sacred, and medicinal attributes besides culinary aspects (Cardone et al., 2020; Das & Sharangi, 2018; Ranjita Devi et al., 2018). Spices are used in foods to impart color, flavor, or aroma (Mardani et al., 2015). Among all, saffron is titled the king of the spices due to its simultaneous coloring, flavoring, and scenting power (Amini et al., 2017; Hosseini et al., 2018; Maggi et al., 2010). Iran, with more than 430 tons of production and an export value of 154,318,000 USD, is the largest producer and exporter of this expensive spice. Spain, Afghanistan, United Arab Emirates, and Greece, with export values of 44,258, 41,931, 10,290, and 6110 thousand USD, respectively, are the top exporters after Iran (Trademap,

Published online: 03 June 2023

2021). Studies show that there are some barriers to expand Iranian saffron export and to compete in the global market (Kabiri et al., 2017; Mardani et al., 2019; Mohamadzadeh Moghadam et al., 2020).

The uncontrolled microbial load of the traditionally dried bulk saffron in the harvest season is one of the export issues (Aghdaie et al., 2012; Milani, 2020). *Enterobacteriaceae*, *Escherichia coli*, and *Clostridium perfringens* are the prevalent microorganisms found in microbial evaluations of saffron (Khazaei et al., 2011). Molds like *Rhizopus* spp. and yeasts have also been reported as frequent contamination factors in saffron (Cosano et al., 2009; Hosseini et al., 2018; Jin et al., 2018). Delayed and improper drying is one of the most important reasons for fungal pollution (Nehvi et al., 2006; Nozad et al., 2016). Although traditional drying methods are being replaced by efficient methods using electric dryers (Ebadi et al., 2015), part of produced bulk saffron is still dried in rural areas in the shade/sun, introducing contamination to the product (Fallahi et al., 2021). Furthermore, there are many microbiological criteria for saffron with different levels of strictness in importing countries. These reasons signify the necessity to find a reliable decontamination method that meets all international standards. Conventional disinfection techniques, including fumigation with sulfur/ethylene oxide, hydrogen peroxide/steam treatments, ozone, heating, or high-pressure processing, have already proved to be ineffective, harmful, or bioactive destructive constituents (Hosseini et al., 2018; Valiasill et al., 2013). Gamma radiation, although effective, is met with a lack of public trust (Castell-Perez & Moreira, 2021).

Plasma is an ionized gas consisting of ions, molecules, free radicals, electrons, and ultraviolet (UV) photons (Liao et al., 2017; Moisan et al., 2001). Cold plasma processing is an emerging green method for the disinfection of heat-sensitive materials. Cold plasma processing is believed to offer many advantages over thermal techniques for decontamination (removal of microbes, toxins, allergens, and pesticides) of many types of fruits, vegetables, grains, nuts, herbs, and spices (Rajan et al., 2023). Herbs and aromatic spices are sensitive to temperatures higher than 40–50 °C due to their volatile compounds; therefore, cold plasma could be a proper decontamination technology (Ebadi et al., 2015; Nozad et al., 2016). It was also reported that essential oil extracted from plasma-treated herbs showed higher antioxidant activity and extraction yield (Rajan et al., 2023). Cold plasma application as a sterilization technology for spices has no background of more than a decade. Studies indicated that low-pressure plasma setups are more suitable for treating 3-dimensional materials like saffron filaments because they can provide a uniform condition and cover the product completely compared to plasma jet, gliding arc, or dielectric-barrier discharge (DBD). In addition, reduced pressure plasma needs low gas amounts, and the feed gas (pure or mixtures) is controllable (Ekezie et al., 2017).

Hosseini et al. (2018) studied the effect of pure oxygen plasma on the three saffron molds. The results indicated that 60-W treatment for 15 min eradicated molds without significant reduction in metabolites (Hosseini et al., 2018). Darvish et al. (2022) also investigated the effect of pure oxygen plasma on saffron decontamination and declared that the highest disinfection level was achieved at 110 W for 30 min (Darvish et al., 2022). None of these studies concern the optimization of the process. Although the decontamination effects of cold plasma treatment have been reported, the mechanism of action is not completely known. The synergistic effects of plasma components (reactive species and UV) play a crucial role in enhancing the efficacy of disinfection (Vassallo et al., 2022). Amini et al. (2017) examined volatile compounds and crocins of saffron after treatment with jet plasma. Pure oxygen in two levels of 5% and 10% was added to pure argon. They reported that the higher the percentage of oxygen, the more bioactive constituents change (Amini et al., 2017). The disinfecting effect of these gas mixtures was not studied in this research. Tabibian et al. (2020) studied the effects of the gliding arc discharge pretreatment on the physicochemical properties of hot air-dried saffron. The results showed that 30 s of pretreatment with 8 kV amplitude indicated the best results in terms of crocin and picrocrocin content after drying (Tabibian et al., 2020).

We used a gas mixture of air, argon, and oxygen in the present study. Since oxygen is an electronegative gas, it decreases the electron density of the plasma and consequently increases the required breakdown voltage. In such a mixture containing oxygen, adding argon can compensate for the consumed electrons and reduces the required input power; therefore, saffron can be treated at lower temperatures. In other words, argon stabilizes the discharge and decreases the overall temperature of the plasma (Dorranian & Alizadeh, 2014).

There are problems to be solved in developing industrial-scale equipment for food processing with cold plasma. A processed product must be harmless and meet the standards criteria for it to be generally recognized as safe (GRAS). The GRAS certificate is a prerequisite to the industrialization of cold plasma. Determining a food's GRAS status requires technical evidence of safety and the basis for concluding that such evidence is well known and accepted. This evidence must be evaluated by a number of independent scientists with relevant experience and scientific background to assess the safety of the food ingredients. Before safety studies, comprehensive evaluations have to be conducted on the effects of plasma processing on the quality and sensory properties of the food ingredients to optimize the process parameters. Different food matrices require specialized optimized processes due to the interactions between plasma and the food being processed (Muhammad et al., 2018).

Collecting more data about this decontamination method can help with the following issues: (1) specializing setup and dosage of the cold plasma treatment for saffron and its industrial-scale up, (2) lowering the safety risk for public health, (3) preventing loss of saffron bioactive constituents (which are used in pharmaceutical and food industries) during the decontamination process, (4) resolving the export issues of this unique product, (5) providing basic information to accelerate food safety organizations' approval/disapproval of plasma treatment. Therefore, in the present study, the radiofrequency low-pressure cold plasma processing of Iranian saffron was optimized to contribute to the industrialization of cold plasma.

Materials and Methods

Biological Materials

Saffron was procured in bulk from Tamim Zarfam Mashreq Zamin Company® (Sarij saffron™ brand). Two lots were obtained: one lot from the harvest season of 2020 (newly harvested and dried saffron) to have a lot with the highest contamination load for getting better disinfecting results; another lot from the 2018 product with the lowest microbial load (no *Escherichia coli*) for inoculation purposes.

The strain of *Escherichia coli* (ATCC® 25922™) was obtained from the microbial strain collection of the Microbiology Department of the Science Faculty, Ferdowsi University of Mashhad.

Plasma Setup and Treatment

A vacuum steel chamber was used in which the capacitively coupled plasma (CCP) was generated by applying a voltage through a radiofrequency power supply (RF 13.56 MHz). This chamber had a diameter of 270 mm and a height of 400 mm. There were two electrodes: the inner electrode or the cathode (on which the sample container was placed), connected to RF power, and the chamber body which was grounded and included RF inlet ports, water inlet pipes for cooling the cathode electrode, and gas inlet ports. The cathode had a diameter of 110 mm, with a negative bias voltage induced. Two quartz windows were placed on either side of the chamber. One was for plasma observation, and the other was for connecting optical emission spectroscopy (OES) collimating lens. The base pressure was about 8 to 10 mTorr, which was provided by a combination of Roots and Rotary vacuum pumps. The working pressure was 12 to 13 mTorr. Treatments began 1 min after reaching the base pressure by turning on the RF power generator in continuous mode. The ratio (%) and the actual percentage of the gas mixture's components (air, oxygen, and argon) are shown in Table 1. The flow rate was 20 standard cubic centimeters per minute (SCCM). The schematic illustration of the plasma setup is presented in Fig. 1. Two batches were separately treated in each experiment to avoid weighing afterward. One batch (0.5 g) was treated for microbial tests and was aseptically transferred to a sterile plate immediately after the treatment. The other batch (5 g) was treated for other physicochemical evaluations and was kept in a dark sealed container in the freezer. For inoculated samples with *E. coli*, treatments were applied separately. The same container (a 100×20-mm glass petri dish) was used for all the experiments.

The Optical Emission Spectroscopy and Sample Temperature Measurement

Reactive species of the plasma discharge were evaluated by spectrophotometer (Avantes, model Avaspec 3648) in the wavelength range of 0 through 2000 nm. The temperature of the container and the samples were determined (average of two readings in 0.5 and 5 g samples) using a thermal imaging infrared camera (Forward-looking infrared device- FLIR, Model E4) from a constant distance (Salehi et al., 2021).

Experimental Design

The central composite design (CCD) of the response surface methodology (RSM) was applied for optimization of the disinfecting process using Design Expert Software ver. 12. Independent variables were determined as two numerical (treatment time, RF power) and one categorical (gas mixture type) variables. Preliminary tests were carried out according

Table 1 Percentage of components of input gas mixtures

Components	Gas mixture name					
	X		Y		Z	
	Ratio %	Actual %	Ratio %	Actual %	Ratio %	Actual %
Air	50	39.06*	65	50.78*	75	58.59*
Oxygen	0	10.48	5	18.62	15	30.71
Argon	50	50.47	30	30.60	10	10.70

*In the actual percentage of the air, the percentages of nitrogen plus trace gases are demonstrated

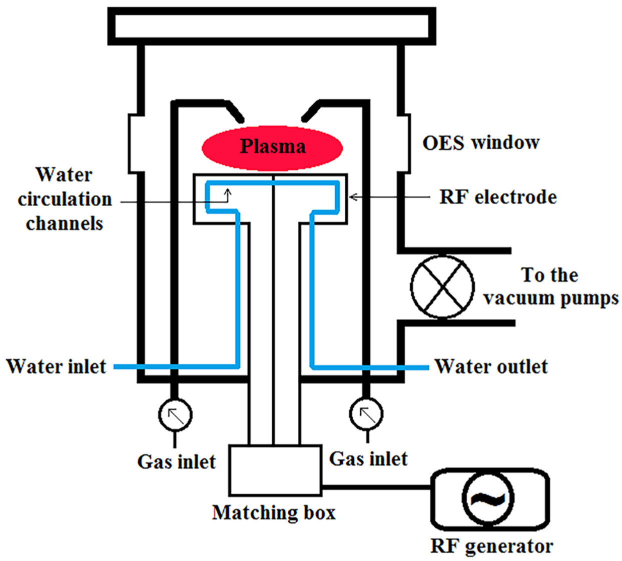

Fig. 1 Schematic illustration of the RF low-pressure cold plasma setup used for saffron decontamination

to the OFAT method and the literature to determine the ranges of variables (Frey et al., 2003). The independent variables' levels in terms of their coded and actual values are presented in Table 2. The design included 12 factorial points (− 1 and + 1 levels), 12 axial points (− α and + α levels), and 18 central points (0 levels) in 2 blocks. A total of 42 experimental runs were conducted to determine the effects of variables on 22 responses including the reduced log of total microorganisms, *coliforms*, molds, and yeasts; the content of crocetin, crocin, picrocrocin, and safranal; coloring strength; aroma; bitterness; the temperature of the saffron sample and its container; reduced moisture; total phenol content; antioxidant activity; color indices (L^*, a^*, b^*, chroma and hue); ΔE_{76} and ΔE_{2000}; and the desirable function.

Microbiological and Physicobiochemical Changes of Saffron

Total Aerobic Mesophilic Microorganisms, *E. coli*, Coliforms, Molds, and Yeast Enumeration

All these microbial tests were carried out simultaneously 1 day after treatments. The initial suspension was prepared by immersing 0.5 g of saffron filaments in 14.5-ml buffered peptone water (BPW) for 1 h to obtain enough inoculum with a uniform distribution of the microorganisms. So, the first dilution was 3×10^{-1} instead of 10^{-1}. The second dilution was made by adding 3 ml of the first dilution (after shaking well) to 7 ml of BPW. Other dilutions were prepared by adding 1 ml of the previous dilution to 9 ml of BPW (ISO, 2017). Total microorganisms were enumerated by pour plate method using plate count agar (PCA) media according to ISO 4833-1 (ISO, 2013). Because of the presence of the motile species in saffron bacteria flora, agar (1%) was added to PCA media. *E. coli* and *coliforms* were enumerated by the pour plate method using CHORMagar ECC differential media, respectively. Incubation for this method was 24 to 48 h at 37 °C. After this time, *E. coli* colonies appeared in blue and *coliforms* in mauve color. Enumeration of molds and yeasts was done by pour plate method using yeast glucose chloramphenicol agar (YGC agar) media as described in ISO 21527-2 (ISO, 2008). Plating was conducted in duplicate for all the above tests.

Inoculation and Enumeration of *Escherichia coli*

As the *E. coli* load in our saffron lot was not high enough (2 log CFU g^{-1} on average) to evaluate plasma efficacy in disinfecting samples with high microbial load, this bacteria was inoculated to a mass of saffron free of it. *E. coli* suspension (0.5 McFarland) was prepared according to Dorranian et al. (2010). The suspension was inoculated to 25 g saffron in a ratio of 1.5 ml:1 g. The inoculated mass was left for 24 h in the laminar air-flow cabinet to dry out and then kept in a refrigerator until treatment. As the microbial load decreases over time, all tests were conducted within 10 days of inoculation (our preliminary tests showed that the microbial load does not change in the meantime).

Determination of Saffron Coloring Strength, Aroma, and Bitterness

The saffron red parts were pulverized and were evaluated for coloring strength, aroma, and bitterness following ISO3636-2 (ISO, 2010).

Quantification of Saffron Major Metabolites

For each treatment, 60 mg of powdered saffron was extracted with 10 ml of 80% ethanol for 25 min by sonication (ultrasonic

Table 2 The independent variables' levels and their coded and actual values

Independent variable		units	Symbol	Coded levels				
				− α	− 1	0	+ 1	+ α
Numerical	RF power	Watt	A	53	60	77	93	100
	Treatment time	minute	B	15	17	23	28	30
Categorical	Gas mixture	(type)	C	Categories				
				X		Y	Z	

bath of BTA Sigma model) at room temperature in darkness. The extract was filtered, and after micro-spinning for 5 min, the supernatant was diluted in 1:6 ratio with HPLC water; then 20 µl of each extract was injected in duplicate into a Knauer chromatography system, equipped with two pumps (model Wellchrom-K1001), PDA detector (model K2800). The column was a Phenomenex RP C_{18} (4.6×250 mm×10 µ). The extract constituents eluted over 55 min. The mobile phase consisted of 0.03%TFA in water (A) and acetonitrile (B) at a flow rate of 1 ml/min with the following gradient: 90% A, 0–5 min; 90–20% A, 5–35 min; 20% A, 35–45 min; 80–100% B, 45–47 min; 100% B, 47–49 min; 100–10% B, 49–50 min and 10% B, 50–55 min. The EZchrom software was used to integrate and calculate the area under the curve. Calculations were performed using the standard calibration curve (Kabiri et al., 2017).

Color Changes

The colorimetric measurements were carried out using a HunterLab MiniScan EZ (Model 4500L, 13 mm aperture, illuminant D65, 10° observer and geometry of 45° a:0°). The values of L^*(lightness/darkness), a^*(redness/greenness), b^*(yellowness/blueness), chroma, and hue parameters were determined in CIE color space from an average of four readings. ΔE_{76} values were calculated using Eq. 1. ΔE_{2000} values were obtained using TECHKON® software (KL, KC, and KH values were considered 1):

$$\Delta E_{76} = \sqrt{\left(L_2^* - L_1^*\right)^2 + \left(a_2^* - a_1^*\right)^2 + \left(b_2^* - b_1^*\right)^2} \tag{1}$$

where L^*_1, a^*_1, and b^*_1 are color indices of the initial sample before the plasma treatment, and L^*_2, a^*_2 and b^*_2 are color indices of the same sample after the treatment.

Visual Evaluation

In order to visually evaluate control and treated saffron samples, digital images were prepared by the image processing system (under controlled conditions). Imaging was done in a chamber with black walls (to prevent light reflection) by a digital camera (Canon EOS 1000D, Taiwan) which was connected to the computer. Seven 10-W fluorescent lamps were used to create light in the chamber where the camera was located, and the light was irradiated to the sample at an angle of 45°. The size of the camera aperture was F/9, shutter speed was 1/5 s, ISO was 100, focus distance was 25 cm, and focal length was 55 mm.

Micromorphological Changes of Saffron Surface

The surface micromorphology of saffron threads and pollens was investigated using a scanning electron microscope (ZEISS, LEO1450vp). The methodology of Hosseini et al. (2018) was employed, and imaging was carried out after coating the threads with a thin layer of gold using an Ion-sputter coater (Hosseini et al., 2018). The samples were observed with 1000×, 2500×, and 5000× magnifications.

Moisture and Volatile Content

Moisture and volatile content of the samples were determined following ISO3636-2 (ISO, 2010). The reduced moisture percentage was calculated by comparing the treated samples with the average of three control samples.

Antioxidant Activity

Extraction and antioxidant activity determination were carried out according to 2,2-diphenyl-1-picrylhydrazyl (DPPH) assay and was expressed as inhibition percentage (Rikabad et al., 2019).

Total Phenol Content

Total phenol content was also determined by the colorimetric method and expressed in ppm of gallic acid (Khodabandeh et al., 2022).

Statistical Analysis

Statistical analysis of the RSM designs was performed using Design Expert software ver. 12. Correlation coefficients were calculated using Minitab software ver. 16.

Results

Microbiological and Physicochemical Changes of Saffron

Results indicated that all plasma factors (time, power, and gas mixture) were effective. Twenty-three responses were analyzed. The order of experiments and response values are shown in Tables 3 and 4. Responses included reduced-log of total aerobic mesophilic microorganisms (ranging from 0.88 through 8.05 log CFU g^{-1}), *coliforms* (0.11–6.71 log CFU g^{-1}), and molds and yeasts (0.21–4.71 log CFU g^{-1}); the amount of crocin (189.54–305.50 ppm), safranal (0.05–0.75 ppm), picrocrocin (56.82–90.07 ppm), crocetin (0.13–1 ppm) content; color strength (170.19–250.45), aroma (27.39–46.7), and bitterness (72.52–88.26); color indices L^* (17.74–21.08), a^* (18.78–28.77), b^* (14.37–21.89), chroma (23.70–39.63), hue (33.65–39.69), ΔE_{76} (1.34–7.29), and ΔE_{2000} (0.71–3.82); antioxidant activity (69.90–84.95%); total phenol content (81.70–119.09 ppm); reduced moisture (29.93–74.67%); container temperature (65–105 °C) and sample temperature (31–47.5 °C). Eleven critical responses

Table 3 Order of experiments in central composite design for the optimization of the cold plasma treatment of saffron

Std	Block	Run	Factor 1 A:Power (Watt)	Factor 2 B:Time (min)	Factor 3 C:Gas mixture (type)	Response 1 Container temperature (°C)	Res. 2 Saffron temperature (°C)	Res. 3 Reduced moisture (%)	Res. 4 Total phenol content (ppm)	Res. 5 Antioxidant activity (%)	Res. 6 L^*	Res. 7 a^*	Res. 8 b^*	Res. 9 Chroma	Res. 10 Hue	Res. 11 ΔE_{2000}
31	1	1	60	28	*Z*	74.00	40.00	33.35	90.23	71.11	19.76	26.07	18.71	32.09	35.66	1.87
1	1	2	60	17	*X*	66.50	31.00	29.93	90.91	75.10	20.23	26.37	17.88	31.86	34.13	1.67
21	1	3	77	23	*Y*	87.50	41.00	51.60	108.30	78.08	19.77	26.43	19.74	32.99	36.76	2.37
33	1	4	77	23	*Z*	90.00	42.50	62.86	106.70	75.76	19.17	25.01	19.62	31.79	38.12	2.54
4	1	5	93	28	*X*	105.00	47.50	50.54	102.73	71.62	18.71	19.18	14.37	23.97	36.84	3.57
32	1	6	93	28	*Z*	102.00	47.50	55.61	101.70	78.59	18.04	20.00	15.27	25.17	37.37	3.19
6	1	7	77	23	*X*	88.00	43.00	60.40	107.05	80.25	20.18	25.82	19.13	32.14	36.52	2.30
19	1	8	77	23	*Y*	89.00	38.50	59.70	103.07	82.12	19.18	22.96	18.32	29.38	38.57	2.67
30	1	9	93	17	*Z*	103.50	44.00	58.33	104.89	84.95	18.24	23.34	17.66	29.26	37.12	2.04
29	1	10	60	17	*Z*	72.00	38.00	40.85	86.25	78.28	19.48	27.26	19.35	33.43	35.37	1.96
18	1	11	93	28	*Y*	99.00	43.50	46.24	98.75	78.79	17.74	20.24	15.52	25.51	37.48	3.11
20	1	12	77	23	*Y*	87.00	43.00	49.61	116.02	82.93	19.14	27.09	20.32	33.86	36.88	2.44
16	1	13	93	17	*Y*	90.00	40.50	43.68	101.82	79.39	18.85	23.59	18.07	29.72	37.45	2.17
35	1	14	77	23	*Z*	91.00	43.00	57.67	87.05	73.84	19.63	26.20	20.02	39.36	39.69	2.54
34	1	15	77	23	*Z*	85.50	39.00	52.34	97.05	80.00	19.30	25.71	20.23	37.58	39.51	2.71
7	1	16	77	23	*X*	84.50	39.00	60.20	94.55	75.66	18.49	25.48	19.28	31.95	37.11	2.09
2	1	17	93	17	*X*	85.00	36.00	36.63	104.66	76.36	18.79	25.08	17.44	30.55	34.82	1.12
3	1	18	60	28	*X*	86.00	40.00	48.86	91.36	74.14	20.61	26.77	19.08	32.89	35.46	2.32
5	1	19	77	23	*X*	86.50	39.00	52.34	119.09	80.51	19.25	25.15	17.89	30.86	35.43	1.48
17	1	20	60	28	*Y*	81.00	39.00	38.67	93.07	73.94	19.07	25.51	17.59	30.99	34.58	1.14
15	1	21	60	17	*Y*	66.50	32.50	30.48	85.00	73.54	20.23	28.77	21.28	35.79	36.49	3.10
25	2	22	77	30	*Y*	90.00	43.00	57.52	109.66	69.90	17.92	23.66	16.62	28.91	35.09	1.38
41	2	23	77	23	*Z*	85.50	39.00	42.89	94.89	78.79	19.40	25.79	19.24	32.18	36.72	2.12
11	2	24	77	30	*X*	92.00	46.00	66.73	110.00	80.78	18.19	22.97	17.24	28.72	36.90	2.03
14	2	25	77	23	*X*	91.50	43.00	52.54	104.66	74.24	21.08	25.88	18.97	32.08	36.24	2.63
38	2	26	77	15	*Z*	85.00	41.00	56.00	88.41	74.75	19.08	26.90	19.30	33.10	35.65	1.86
12	2	27	77	23	*X*	80.00	38.50	38.37	86.25	77.98	19.99	25.37	18.43	31.36	35.99	1.97
42	2	28	77	23	*Z*	86.50	41.00	53.58	90.34	72.83	19.86	26.61	20.80	33.77	37.97	2.96
23	2	29	100	23	*Y*	96.50	43.00	63.59	95.57	75.05	19.19	21.82	17.23	27.80	38.30	2.77
10	2	30	77	15	*X*	85.00	42.50	69.53	111.02	77.17	19.89	26.13	17.52	31.47	33.80	1.36
36	2	31	53	23	*Z*	72.00	34.50	41.50	81.70	70.81	19.92	27.76	19.87	34.14	35.60	2.54
9	2	32	100	23	*X*	101.50	43.50	74.67	95.34	79.19	18.19	18.78	14.46	23.70	37.59	3.82
37	2	33	100	23	*Z*	95.00	43.50	67.51	103.52	76.57	18.01	20.44	15.57	25.70	37.30	2.98
24	2	34	77	15	*Y*	66.50	36.00	74.25	102.95	72.83	18.81	25.35	16.87	30.45	33.65	0.71

Table 3 (continued)

Std	Block	Run	Factor 1 A:Power (Watt)	Factor 2 B:Time (min)	Factor 3 C:Gas mixture (type)	Response 1 Container temperature (°C)	Res. 2 Saffron temperature (°C)	Res. 3 Reduced moisture (%)	Res. 4 Total phenol content (ppm)	Res. 5 Antioxidant activity (%)	Res. 6 L^*	Res. 7 a^*	Res. 8 b^*	Res. 9 Chroma	Res. 10 Hue	Res. 11 ΔE_{2000}
8	2	35	53	23	*X*	66.00	34.00	42.86	89.77	76.57	20.03	27.63	19.65	33.91	35.41	2.28
28	2	36	77	23	*Y*	80.50	38.00	39.48	91.36	77.58	20.02	25.96	19.78	32.63	37.30	2.57
26	2	37	77	23	*Y*	82.00	39.00	51.55	91.82	78.18	19.46	26.76	20.03	31.99	36.98	2.39
40	2	38	77	23	*Z*	88.00	39.50	59.72	115.23	83.33	19.42	26.41	20.83	33.63	38.27	2.92
39	2	39	77	30	*Z*	98.00	43.00	68.77	109.43	76.87	18.28	23.35	16.83	28.79	35.79	1.63
22	2	40	53	23	*Y*	65.00	33.50	33.93	81.70	73.13	20.71	28.07	20.46	34.73	36.09	2.90
13	2	41	77	23	*X*	85.50	41.50	54.30	97.95	80.40	20.86	25.67	19.21	32.07	36.81	2.67
27	2	42	77	23	*Y*	86.50	41.50	57.01	101.25	72.32	19.54	27.12	21.89	34.85	38.90	3.42

The ratio (%) of air, oxygen, and argon, respectively, in gas mixtures: X (50:0:50), Y (65:5:30), and Z (75:15:10)

(responses 12 through 22) that determine the final quality of saffron (Table 3) were selected based on previous studies (Darvish et al., 2022; Hosseini et al., 2018; Tabibian et al., 2020) to calculate the desirable function (the twenty-third response) as a comprehensive approach for optimization. Fitted models for all responses were significant, and their lack of fit was insignificant in the 5% confidence level. The *P*-values of the models and lack of fits; the *F*-values of the models, independent variables, two-factor-interaction, and quadratic terms; standard deviation; *R*-squared; adjusted *R*-squared; and predicted *R*-squared and the adequate precision values of the mentioned responses are demonstrated in Tables 9 and 10. The mathematical modeling for all the responses (except for the desirable function which equation is presented in Table 5) was done and after removing all non-significant factors, the coded polynomial equations are as follows (Eqs. 2–23):

$$\textit{Container temperature} = +85.67 + 11.07\,A + 5.21\,B + 0.2619\,C_1 - 2.31\,C_2 \tag{2}$$

$$\textit{Saffron temperature} = +40.88 + 3.25\,A + 2.22\,B - 1.05\,A^2 \tag{3}$$

$$\textit{Reduced moisture}^{0.83} = +26.49 + 3.44\,A \tag{4}$$

$$\textit{Antioxidant activity}^{-1.16} = +0.0065 - 0.0002\,A \tag{5}$$

$$\textit{Total phenl}^{-3} = +(9.962E-07) - (2.270E-07)A + (1.839E-07)A^2 \tag{6}$$

$$L^* = +19.58 - 0.6855\,A - 0.2787\,B + 0.2807\,C_1 - 0.0678\,C_2 - 0.4385\,B^2 \tag{7}$$

$$a^* = +25.86 - 2.54\,A - 1.19\,B - 0.7111\,AB - 0.9011\,A^2 + 0.5789\,B^2 \tag{8}$$

$$b^* = +19.65 - 1.40\,A - 0.6401\,B - 0.6174\,C_1 + 0.3234\,C_2 - 0.8763\,A^2 - 1.11\,B^2 \tag{9}$$

$$\textit{Chroma} = +33.03 - 2.88\,A - 1.34\,B - 0.8221\,C_1 + 0.0400\,C_2 - 0.8763\,A^2 - 1.11\,B^2 \tag{10}$$

$$\textit{Hue} = +37.43 + 0.7501\,A + 0.3595\,B - 0.6800\,C_1 + 0.1393\,C_2 + 0.6072\,BC_1 - 0.3400\,BC_2 - 0.3250\,A^2 - 1.11\,B^2 \tag{11}$$

$$\Delta E_{2000} = +2.49 + 0.2398\,A + 0.1962\,B - 0.1043\,C_1 + 0.0264\,C_2 + 0.4950\,AB + 0.3097\,BC_1 - 0.2053\,BC_2 + 0.2175\,A^2 - 0.4758\,B^2 \tag{12}$$

Table 4 Order of experiments in central composite design for the optimization of the cold plasma treatment of saffron

Std	Block	Run	Factor 1 A:Power (Watt)	Factor 2 B:Time (min)	Factor 3 C:Gas Mixture (type)	Response 12 Total microorganisms reduced log (log CFU g^{-1})	Res. 13 *Coliforms* reduced log (log CFU g^{-1})	Res. 14 Molds & yeasts reduced log (log CFU g^{-1})	Res. 15 Crocin (ppm)	Res. 16 Safranal (ppm)	Res. 17 Picrocrocin (ppm)	Res. 18 Crocetin (ppm)	Res. 19 Coloring strength	Res. 20 Aroma	Res. 21 Bitterness	Res. 22 ΔE_{76}	Res. 23 Desirable function
34	1	1	77	23	*Z*	3.70	4.11	2.62	270.00	0.31	77.12	0.35	243.24	38.37	86.83	4.14	52.58
16	1	2	93	17	*Y*	4.13	4.63	2.34	267.49	0.59	64.30	0.44	212.13	39.28	82.34	2.98	59.20
20	1	3	77	23	*Y*	5.74	6.71	3.23	283.29	0.23	76.74	0.36	224.43	36.55	80.67	4.37	59.84
5	1	4	77	23	*X*	4.71	5.23	2.48	286.45	0.27	81.43	0.31	206.00	35.08	79.35	2.04	58.12
21	1	5	77	23	*Y*	4.85	6.71	3.25	270.10	0.23	69.18	0.30	224.26	37.94	81.02	3.87	56.94
4	1	6	93	28	*X*	8.05	6.71	4.71	220.74	0.75	58.32	0.97	187.92	44.82	81.19	6.94	75.02
19	1	7	77	23	*Y*	5.27	6.71	4.71	256.90	0.21	70.76	0.28	233.59	36.42	84.44	3.69	59.34
7	1	8	77	23	*X*	4.77	5.23	2.48	291.75	0.42	76.14	0.40	199.38	30.65	78.44	3.08	59.74
29	1	9	60	17	*Z*	1.31	0.86	1.53	282.91	0.18	77.62	0.33	218.61	33.67	86.94	3.64	39.16
3	1	10	60	28	*X*	3.02	4.58	3.23	300.74	0.36	79.89	0.35	223.28	33.48	82.49	3.81	56.10
30	1	11	93	17	*Z*	4.63	6.71	2.70	266.43	0.34	61.80	0.35	206.33	39.18	84.44	2.90	58.06
18	1	12	93	28	*Y*	6.57	6.71	4.71	236.30	0.68	56.82	1.00	202.15	43.90	79.72	5.68	72.26
35	1	13	77	23	*Z*	4.87	6.71	2.68	270.50	0.15	73.63	0.25	230.87	37.89	82.62	4.05	54.51
1	1	14	60	17	*X*	0.88	0.59	0.82	293.28	0.16	80.85	0.35	219.95	31.27	86.72	2.62	38.38
31	1	15	60	28	*Z*	2.75	3.42	2.30	276.34	0.30	76.74	0.28	245.45	39.10	86.86	2.91	49.97
17	1	16	60	28	*Y*	3.79	3.65	3.71	279.57	0.28	76.53	0.28	232.67	37.66	85.73	1.62	56.57
32	1	17	93	28	*Z*	6.73	6.71	4.71	233.19	0.43	59.52	0.75	196.72	42.52	75.18	5.93	65.62
2	1	18	93	17	*X*	5.04	6.71	1.63	277.11	0.39	66.86	0.32	205.80	32.89	80.13	1.54	61.66
6	1	19	77	23	*X*	4.58	5.23	4.71	272.23	0.21	73.70	0.36	218.16	38.32	80.67	3.48	57.28
33	1	20	77	23	*Z*	4.04	5.98	4.71	257.56	0.21	70.76	0.28	234.92	42.28	84.66	3.62	56.41
15	1	21	60	17	*Y*	2.04	3.07	0.56	305.50	0.17	90.07	0.19	228.38	34.03	83.56	6.16	42.94
14	2	22	77	23	*X*	5.28	6.71	3.97	276.58	0.22	74.77	0.34	203.62	37.13	75.50	3.93	59.65
37	2	23	100	23	*Z*	8.05	6.71	3.08	189.54	0.31	59.70	0.67	180.51	37.68	73.52	5.46	59.95
12	2	24	77	23	*X*	4.01	4.03	3.97	259.20	0.28	71.61	0.21	205.33	36.10	81.98	2.84	53.31
27	2	25	77	23	*Y*	6.16	6.71	4.71	275.82	0.23	84.10	0.36	221.88	39.05	82.45	5.94	63.13
10	2	26	77	15	*X*	3.00	3.72	3.06	281.82	0.36	68.78	0.40	198.33	27.54	76.75	2.09	54.12
40	2	27	77	23	*Z*	4.05	3.70	3.97	263.66	0.14	70.21	0.31	231.32	38.45	83.72	4.78	49.18
26	2	28	77	23	*Y*	5.79	5.06	3.55	252.03	0.15	71.92	0.21	218.71	34.89	79.56	3.46	53.44
39	2	29	77	30	*Z*	4.38	5.23	3.73	265.15	0.60	66.00	0.45	204.37	37.55	79.89	2.58	63.83
28	2	30	77	23	*Y*	4.82	5.97	3.97	269.38	0.15	75.97	0.36	223.69	34.06	82.62	3.97	56.21
25	2	31	77	30	*Y*	6.10	6.71	4.71	269.89	0.36	70.50	0.30	195.56	31.54	76.15	2.25	65.74
13	2	32	77	23	*X*	4.25	6.71	3.97	257.47	0.15	69.26	0.29	203.49	33.22	77.87	3.96	54.71
8	2	33	53	23	*X*	1.46	1.20	1.11	297.80	0.14	84.07	0.18	223.19	36.06	88.26	4.24	38.64
11	2	34	77	30	*X*	5.18	6.71	4.71	265.71	0.56	67.82	0.31	190.65	33.50	74.92	3.05	67.06
22	2	35	53	23	*Y*	1.91	1.78	1.69	286.37	0.12	82.78	0.25	218.31	29.57	86.08	5.36	40.04
38	2	36	77	15	*Z*	2.39	2.00	2.90	296.73	0.42	80.17	0.39	215.59	31.10	81.49	3.34	51.67
41	2	37	77	23	*Z*	4.42	6.71	3.97	283.05	0.22	79.23	0.27	216.98	37.95	83.23	3.22	59.49
23	2	38	100	23	*Y*	6.57	6.71	3.06	221.87	0.73	57.73	0.98	170.19	35.23	72.52	4.26	70.13

Table 4 (continued)

Std	Block	Run	Factor 1 A:Power (Watt)	Factor 2 B:Time (min)	Factor 3 C:Gas Mixture (type)	Response 12 Total microorganisms reduced log (log CFU g^{-1})	Res. 13 *Coliforms* reduced log (log CFU g^{-1})	Res. 14 Molds & yeasts reduced log (log CFU g^{-1})	Res. 15 Crocin (ppm)	Res. 16 Safranal (ppm)	Res. 17 Picrocrocin (ppm)	Res. 18 Crocetin (ppm)	Res. 19 Coloring strength	Res. 20 Aroma	Res. 21 Bitterness	Res. 22 ΔE_{76}	Res. 23 Desirable function
42	2	39	77	23	Z	5.11	6.71	4.71	265.58	0.16	72.78	0.23	212.94	35.32	80.61	4.90	57.52
24	2	40	77	15	Y	1.05	0.11	0.21	290.79	0.30	81.59	0.28	207.61	30.58	81.37	0.98	45.41
9	2	41	100	23	X	8.05	6.71	2.86	229.08	0.71	58.79	0.84	190.46	46.70	86.28	7.29	70.52
36	2	42	53	23	Z	1.88	1.82	1.18	256.61	0.05	76.47	0.13	201.07	27.39	79.34	4.44	35.08

$$\begin{aligned}&\textit{Total microorganisms reduced log}\\&\quad = +4.74 + 1.92\,A + 1.08\,B + 0.0348\,C_1 + 0.2140\,C_2\end{aligned} \tag{13}$$

$$\begin{aligned}\textit{Coliforms reduced log}^{1.02} = &+6.04 + 1.91\,A\\&+1.19\,B - 0.7671\,A^2 - 0.8054\,B^2\end{aligned} \tag{14}$$

$$\begin{aligned}\textit{Mold and yeast reduced log}^{0.63} = &+2.29 + 0.3075\,A + 0.4501\,B\\&- 0.0125\,C_1 - 0.0219\,C_2 - 0.0253\,BC_1\\&+ 0.2701\,BC_2 - 0.3414\,A^2 - 0.1421\,B^2\end{aligned} \tag{15}$$

$$\begin{aligned}\textit{Crocin} = &+270.09 - 21.68\,A\\&- 10.12\,B + 4.22\,C_1 + 1.03\,C_2\\&- 7.98\,AB - 9.77\,A^2 + 5.97\,B^2\end{aligned} \tag{16}$$

$$\begin{aligned}\textit{Picrocrocin}^{-3} = &(+2.469E-06) + (1.154E-06)A\\&+ (3.621E-07)B + (2.404E-07)AB\\&+ (5.048E-07)A^2 + (1.624E-07)B^2\end{aligned} \tag{17}$$

$$\begin{aligned}\textit{Safranal}^{0.75} = &+0.3173 + 0.1536\,A\\&+ 0.0626\,B + 0.0403\,C_1\\&+ 0.0002\,C_2 + 0.0154\,AC_1\\&+ 0.0466\,AC_2 + 0.0520\,A^2 + 0.1077\,B^2\end{aligned} \tag{18}$$

$$\begin{aligned}\textit{Crocetin}^{0.22} = &+0.7672 + 0.0796\,A + 0.229\,B\\&+ 0.0409\,AB + 0.0321\,A^2 + 0.0180\,B^2\end{aligned} \tag{19}$$

$$\begin{aligned}\textit{Coloring strength} = &+219.60 - 12.53\,A\\&- 1.95\,B - 7.18\,C_1 + 2.68\,C_2\\&- 5.99\,AB - 7.33\,A^2 - 4.97\,B^2\end{aligned} \tag{20}$$

$$\textit{Aroma} = +36.88 + 2.96\,A + 2.09\,B - 1.38\,B^2 \tag{21}$$

$$\begin{aligned}\textit{Bitterness}^{2.55} = &+74226.16 - 7100.37\,A\\&- 2370.74\,B - 2549.93\,C_1 + 304.10\,C_2\end{aligned} \tag{22}$$

$$\begin{aligned}\Delta E_{76}{}^{0.83} = &+3.05 + 0.2448\,A + 0.2570\,B\\&- 0.1438\,C_1 + 0.0285\,C_2 + 0.8324\,AB\\&+ 0.4103\,BC_1 - 0.2434\,BC_2 + 0.4434\,A^2 - 0.4877\,B^2\end{aligned} \tag{23}$$

where A, B, and C are power, time, and gas mixture, respectively.

In the case of decontamination of inoculated samples with *E. coli*, the results were not included in the design because all of the 42 treatments could eradicate *E. coli* bacteria. The

Table 5 ANOVA for the linear model of desirability function

Source	Sum of squares	*df*	Mean square	*F*-value	*p*-value	
Block	27372.68	1	27372.68			
Model	1.077E+07	4	2.692E+06	74.31	< 0.0001	Significant
A-Power	7.392E+06	1	7.392E+06	204.06	< 0.0001	
B-Time	2.926E+06	1	2.926E+06	80.77	< 0.0001	
C-Gas mixture	4.489E+05	2	2.245E+05	6.20	0.0049	
Residual	1.304E+06	36	36224.09			
Lack of fit	7.833E+05	24	32635.57	0.7520	0.7343	Not significant
Pure error	5.208E+05	12	43401.12			
Cor total	1.210E+07	41				

Desirable Function$^{1.86}$ = 1834.34 + 554.97 A + 349.16 B + 82.67 C_1 + 63.11 C_2

average microbial load of the inoculated sample with *E. coli* (positive control) was 6.07 log CFU g^{-1}.

The analyses of the 3D plots (not shown except for the desirable function response, Fig. 2) showed that the highest values of the total microorganisms reduced log, *coliforms* reduced log, safranal, crocetin, aroma, ΔE_{76}, ΔE_{2000}, container temperature, saffron temperature, and desirable function were obtained when the plasma treatment power and time factors were at their highest levels (93 W and 28 min, respectively). The highest value of molds and yeasts reduced log was obtained at the high level of power (≈ 85 W) and the highest level of time. The highest levels of crocin, picrocrocin, and bitterness were obtained when the power and time factors were at or near the lowest levels (60 W and 17 min, respectively). The highest value of coloring strength was obtained at the lowest power level and high level of time (≈ 25 min). The highest values of L* and b* were obtained at the lowest power level and low to moderate level of time. The highest values of a* and chroma were obtained at the lowest power level and low level of time. Regarding the hue response, the highest value was obtained at the highest power level, a high level of time for the X mixture and a moderate level of time (≈ 23 min) for the Y and Z mixtures. The highest values of reduced moisture, total phenol, and antioxidant activity were obtained at the lowest time level (power did not affect these responses).

Furthermore, the disinfection capacity of the gas mixtures was compared using 3D plots. The capacity of the gas mixtures for the decontamination of total aerobic mesophilic microorganisms was in the following order: $Y<Z<X$. For the decontamination of the *coliforms*, the capacity of the gas mixtures was approximately equal. In the case of decontamination of molds and yeasts, gas mixture Y was notably better than X and Z mixtures. And X mixture had a higher log-reduction of molds and yeast than Z and was also the best mixture in terms of crocin and safranal responses; although it indicated the highest values of color change (ΔE_{76} and ΔE_{2000}). Regarding the coloring strength and bitterness, the Z mixture was the best, although it showed the highest value of container temperature. The gas mixture type had no significant effect on nine responses, including *coliforms* reduced log, picrocrocin, crocetin, aroma, a*, saffron temperature, reduced moisture, total phenol, and antioxidant activity (as can be seen in Tables 9 and 10, the independent variable "gas mixture" was not included in these responses' models).

To find the best condition which leads to the highest decontamination and the lowest changes in secondary metabolites, it was necessary to make proper compromises between opposing eleven critical responses involved in the second design. So, a twelfth response, the desirable function, was calculated and analyzed. This approach is common in multi-objective optimization processes (Pandey et al., 2018). Responses that were directly proportional to the desirable function were normalized to their maximum value, while responses that were inversely related to the desirable function and their increase that was undesirable (color changes) should be inverted before normalization. The desirable function equation was defined by summing up responses after assigning different weights (coefficients) to them based on their importance and effectiveness on the outcome (Hosseinian et al., 2020). The desirable function (D.F.) formula was calculated for each experiment and expressed in the desirability percentage (Eq. 24).

$$\text{D.F.\%} = \frac{\Sigma 12\,\Delta\left(\frac{a_i}{A}\right) + 12\,\Delta\left(\frac{b_i}{B}\right) + 8\,\Delta\left(\frac{c_i}{C}\right) + 12\,\Delta\left(\frac{d_i}{D}\right) + 12\,\Delta\left(\frac{e_i}{E}\right) + 11\,\Delta\left(\frac{f_i}{F}\right) + 8\,\Delta\left(\frac{g_i}{G}\right) + 5\,\Delta\left(\frac{h_i}{H}\right) + 5\,\Delta\left(\frac{i_i}{I}\right) + 5\,\Delta\left(\frac{j_i}{J}\right) + 10\,\Delta\left(\frac{1}{k_i}\right)}{100} \tag{24}$$

where i is the number of the run order; a is the reduced logs of the total microorganisms; b is the reduced logs of *coliforms*, c is the reduced logs of molds and yeasts; d is the crocin content, e is the safranal content, f is the picrocrocin

Fig. 2 **a**–**c** are three-dimension response surface plots of the effects of the time and power on the desirable function in three gas mixtures of *X*, *Y*, and *Z*, respectively

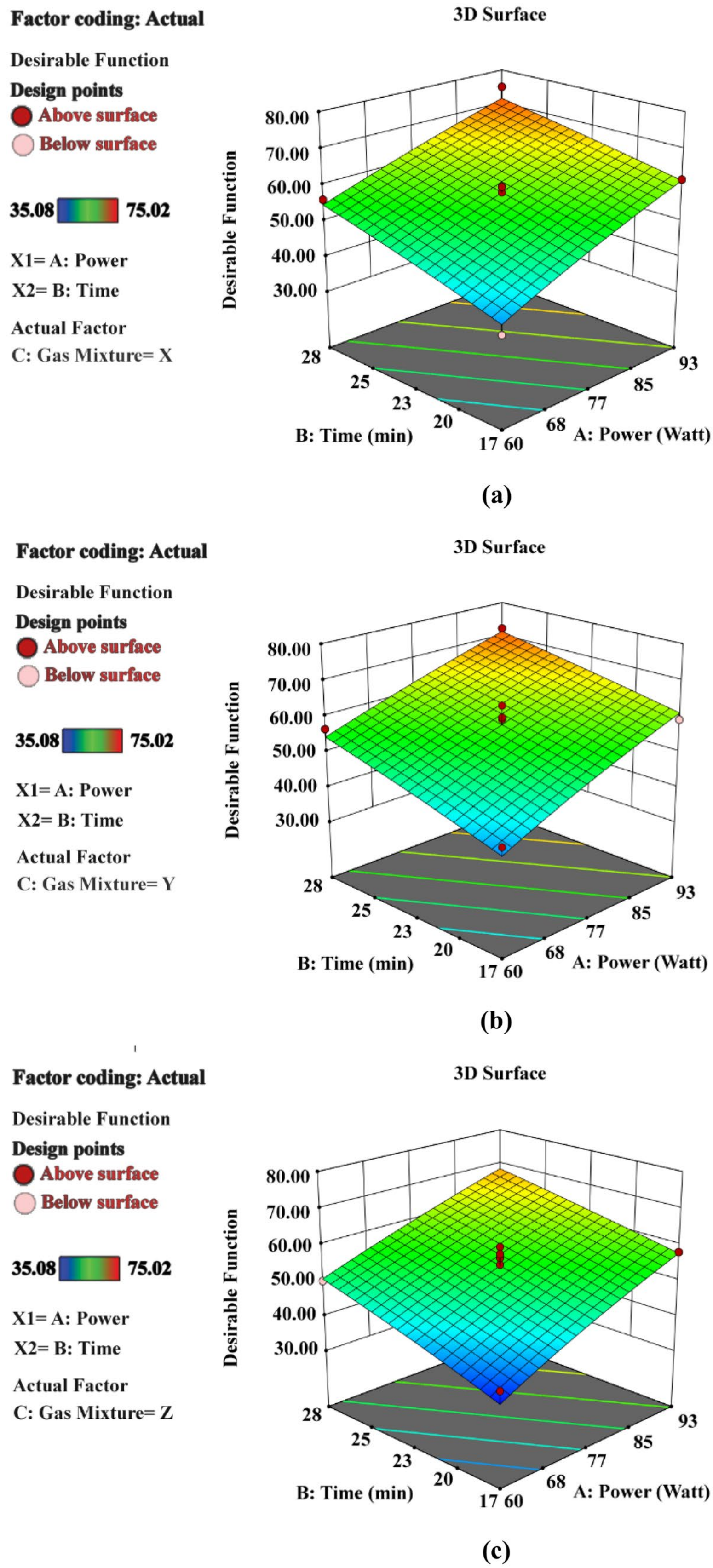

content, g is the crocetin content; h is the coloring strength, i is the aroma, j is the bitterness, and k is the ΔE_{76}.

To avoid confusion, only the 3D plots (Fig. 2) and the analysis of variance (ANOVA) table of the desirable function response (our main comprehensive response) are presented here (Table 4). The linear model was fitted for the desirable function data and was significant with an accuracy of 99%. The lack of fit of the model was insignificant (p-value 0.73). Results proved that all three factors significantly affected the desirable function at 1% confidence level, but interactions between factors were insignificant. The mathematical modeling for the desirable function was done, and the coded equation is shown beneath Table 5. The positive power (1.86) of the Desirable function eq (Table 5) indicates that the higher desirability occurs at the higher areas of the curves (Fig. 2).

As illustrated in Fig. 2, the three-dimensional response surface plots were plotted for desirable function response to study the effect of "treatment time" and "RF power" in three gas mixtures (X, Y, and Z). In the 3D graphs, Y-axis shows the "desirable function" response (dependent variable), the X-axis and Z-axis indicate "treatment time" and "RF power" (independent variables), respectively. In all of the 3D graphs, by the increase in the treatment time and the power of RF plasma, the desirable function was increased. The highest values of the desirable function response observed in X, Y, and Z gas mixtures were 75.02%, 72.26%, and 65.62%, respectively. Therefore, the X mixture was better than the Y mixture in terms of the desirable function and both were notably better than the Z mixture. The lowest values of the desirable function response were observed at the lowest treatment time and power level. The parallel lines at the bottom of the 3D plots that are in fact contour plots (2D) show that there are no interaction effects involved in the modeling.

Micromorphological Changes of Saffron surface

A sample treated with one of the highest levels of power and time (93 W for 28 min) and the Z gas mixture (containing the highest level of oxygen) was studied against an untreated sample (control). The texture changes were evaluated in three levels of magnifications (1000×, 2500×, and 5000×) to inspect different aspects of the microstructures of the saffron thread (Fig. 3). As can be observed, the surface of the treated saffron thread is obviously destructed. In the treated sample (Fig. 3a) at 1000×, in comparison to control (Fig. 3b), the thread cellular pattern of the epidermal cells is somehow softened and barely diagnosable, and the interstices structures are almost gone. At 2500×, there are evident damages to some protrusions in treated sample (marked in Fig. 3c) compared to untreated sample (Fig. 3d). The etching of the surface of the treated sample (Fig. 3e) is best observed at 5000× which the surface is scratched

Fig. 3 SEM images of saffron threads and pollens in plasma-treated and control samples, sections: **a**, **c** and **e** are 1000×, 2500×, 5000× magnifications of the treated saffron thread; **b**, **d**, and **f** are the control saffron thread; **g** and **f** are treated and control pollen, respectively ▸

in contrast to the surface of the control sample, which is completely smooth (Fig. 3f). Some pollens were detected on the stigmas. So, the plasma effect on the pollens' surface was also evaluated in the treated (Fig. 3g) and control (Fig. 3h) samples. At the highest magnification of 5000×, no apparent changes were observed in the pollens after the plasma treatment.

Optimum Conditions for Plasma Treatment of Saffron and Its Validation

Optimization and validation of the process were conducted according to Pandey et al. (2018). For this purpose, the goals of the factors and responses were set according to saffron standards (Table 6).

After setting the goals, the software generated twenty solutions, of which the first solution suggested the application of gas mixture "Y", 76 Watt of power for 26 min, with the desirable function of 63%. Under the optimized conditions (Y gas mixture, 76 W for 26 min), samples were treated and evaluated for the studied traits in three replications. CV% values for the experimental values ranged from 0 to 11.53%, indicating that the designed model was well-fitted and appropriate for predicting the optimal condition (Table 7).

Optical Emission Spectroscopy of Plasma and Measuring Sample Temperature

The OES graphs of the optimal treatment (in 0.5 and 5 g samples) are presented in Fig. 4. The wavelengths of 1–400 nm are in the UV range and the wavelengths of 380–780 nm are in the visible spectrum. Each peak represents one reactive species.

The prominent peaks with high intensities were identified using similar studies. Figures show the plasma spectroscopy of the Y gas mixture under optimized conditions. Characteristic peaks at the 696–853 nm wavelength range correspond to Ar plasma (Ar^+ species). In oxygen plasma, OES spectra unique peaks are around 770, 840-nm wavelength associated with monoatomic oxygen, and peaks around 560, 525, 598, 638, and 677 nm wavelength are attributed to O_2^+, O^+ ions. Spectral lines 335 and 380–400 nm are in accordance with excited N_2 species and N_2^+ ions, respectively. Two peaks that had the highest intensity in the OES graphs were in the range of the UV light (388) and the pink-purple section of the visible spectrum (748); so, the visible color of the resulted plasma was pink-purple

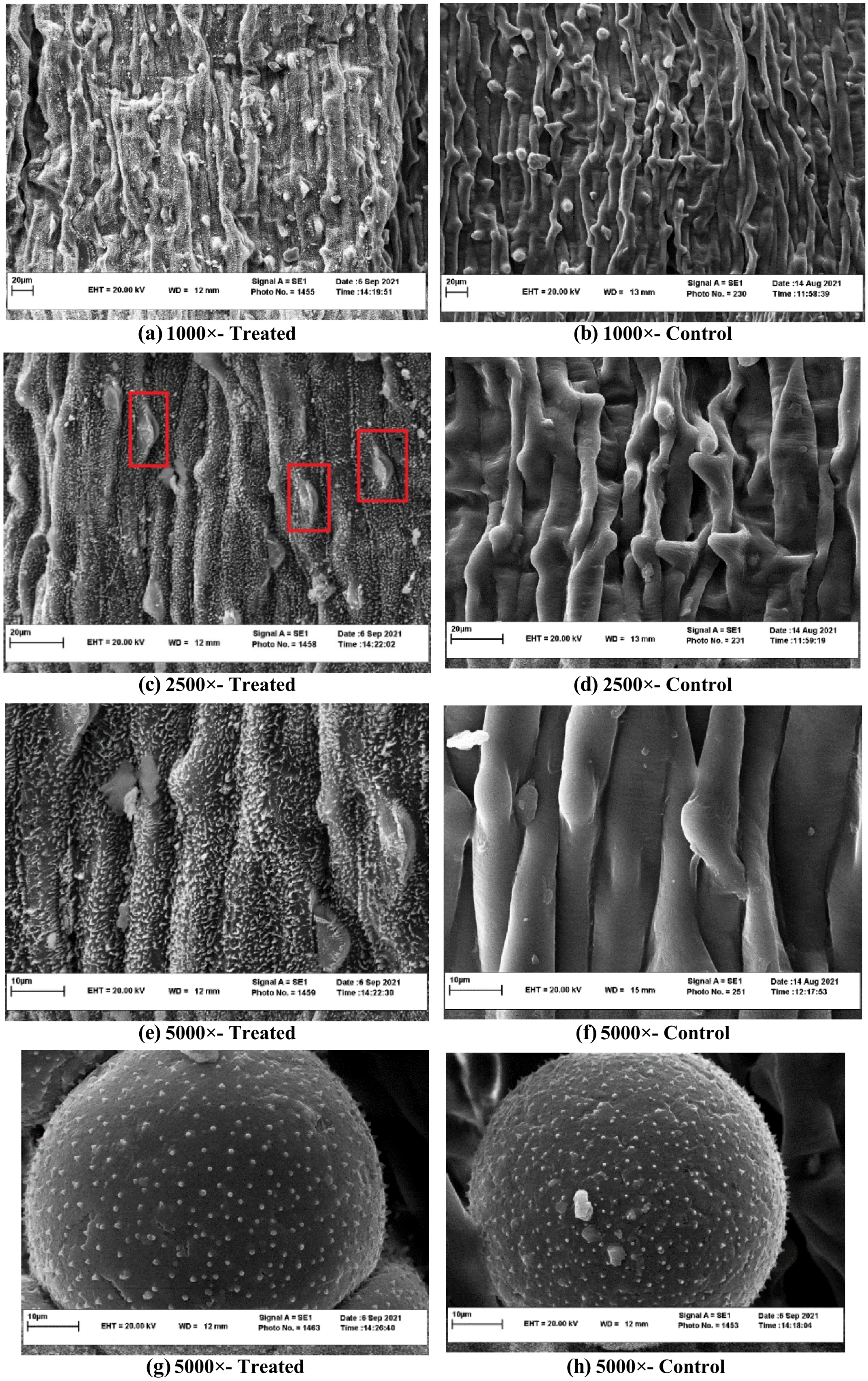
(a) 1000×- Treated
(b) 1000×- Control
(c) 2500×- Treated
(d) 2500×- Control
(e) 5000×- Treated
(f) 5000×- Control
(g) 5000×- Treated
(h) 5000×- Control

Table 6 Goals for the factors and responses in optimization

Factors and responses	Goal
Power, time and gas mixture	In range
Microbiological and phyto-chemical responses	Target to: upper level
Coloring strength	In range (min:190-max: upper level)
Aroma and bitterness	In range
ΔE_{76} (color change)	In range (min: lower level-max: 4)
Desirable function	Target to: upper level

(Fig. 5a). The samples' temperature and container were also measured right after the plasma treatments using thermalimaging infrared camera (Fig. 5b). For the optimal treatment, the average temperature of the samples was 40 °C (in 0.5 g) and 44 °C (in 5 g). The average temperature of their container was 89 °C (in 0.5 g) and 87 °C (in 5 g).

Correlations

To determine correlation coefficients, all responses were analyzed together. There were strong correlations among metabolite content (Table 8). Picrocrocin had a strong positive correlation (0.83) with crocin and negative correlations with crocetin and safranal with coefficients of − 0.73 and − 0.68, respectively. Crocetin content was negatively correlated with crocin ($R^2 = -0.69$), while showed a strong positive correlation (0.81) with safranal. The correlations between power and the contents of crocin, safranal, picrocrocin, and crocetin were − 0.70, 0.66, − 0.82, and 0.71, respectively. Power also showed a positive correlation with the reduced log of *coliforms* (0.67). A high correlation was observed between the reduced log of molds/yeasts and reduced log of *coliforms* (0.72) and reduced log of total microorganisms (0.67). The R^2 values for correlations of coloring strength with bitterness (0.80) and picrocrocin (0.60) were highly positive. Mild positive correlations were also detected between ΔE_{76} and crocetin (0.49) and aroma (0.51). The container and sample temperature were highly correlated with power and poorly correlated with time. Strong positive correlations were observed among temperatures and reduced microbial load. Also, a moderate positive correlation existed between container temperature and the contents of crocin, crocetin, safranal, and aroma. There was a strong negative correlation between picrocrocin and the temperature of the container and samples. The a* and b* indices showed positive correlations with the contents of picrocrocin and crocin and a negative correlation with crocetin and safranal. The a* also was positively correlated with *L** (0.72) and coloring strength (0.61). The reduced moisture had a moderate positive correlation with sample temperature.

Table 7 The predicted values of the optimal condition and its experimental values for validation

	Total microorganisms reduced log	*Coliform* reduced log	Molds and yeasts reduced log	Crocin	Safranal	Picrocrocin	Crocetin	Coloring strength	Aroma	Bitterness	ΔE_{76}	Desirable function
A. Predicted values of the solution	6.00	6.71	4.71	264.24	0.26	70.54	0.35	218.96	36.75	80.88	3.61	62.65
B. Experimental values	5.75	6.71	4.00	267.43	0.30	71.45	0.32	210.65	35.34	79.39	3.92	61.22
CV%	3.01	0	11.53	0.85	10.10	0.91	6.33	2.74	2.77	1.31	5.82	1.63

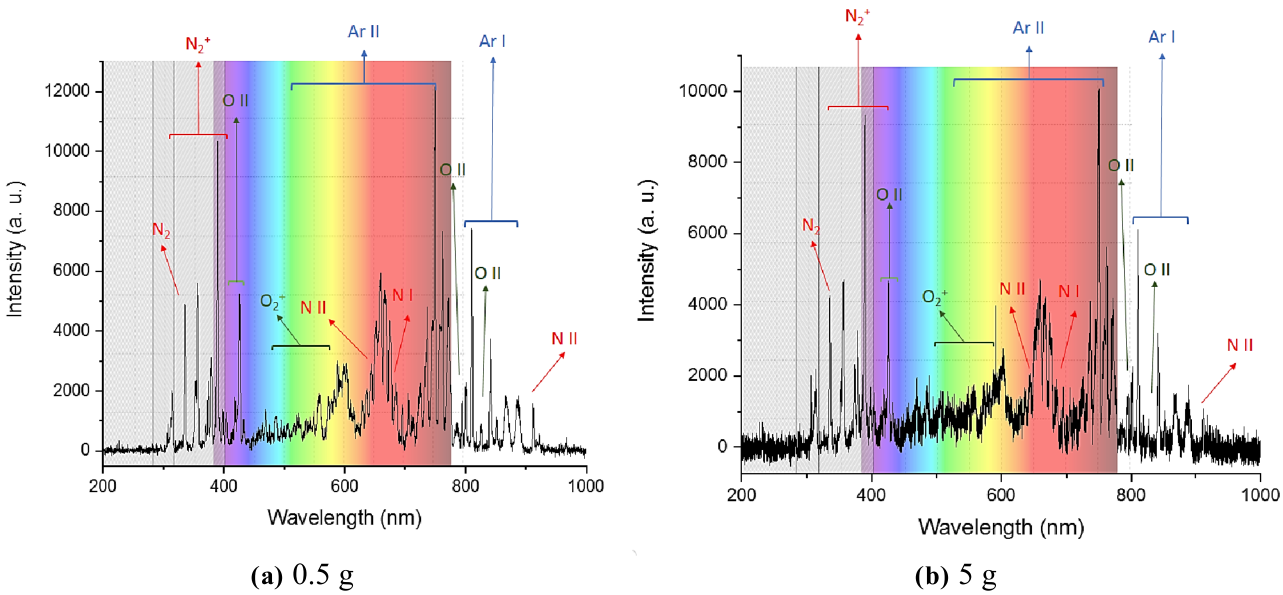

Fig. 4 The OES graphs of the best treatment in two samples and their main reactive species: **a** 0.5, g **b** 5 g

Discussion

The quality of saffron is determined by its color, odor, and taste (Azarabadi & Özdemir, 2018). Based on ISO 3236-1 specification and the national standard of Iran (No. 259-1), our initial sample quality with an average coloring strength value of 219.62, aroma of 32.91, and bitterness of 86.90 fell into category I (Tables 11 and 12) (INSO, 2013; ISO, 2011). We observed that with increasing the time and power of plasma, the coloring strength and bitterness of saffron decreased but the aroma increased. Nevertheless, optimization goals were set so that the quality of the samples treated with optimal conditions was maintained in the same range as the initial sample. At the optimal conditions, the samples' average coloring strength, aroma, and bitterness were 210.65, 35.34, and 79.39, respectively.

As the three major indices of saffron quality (coloring strength, aroma, and bitterness) would not be determined unless tested in the laboratory, the first commercial quality control of saffron is the color acceptability in the market, and it is done visually (Mohamadzadeh Moghadam et al., 2020). The red color of saffron is indicative of its crocin content (Fallahi et al., 2021). Plasma treatment changes the color of the saffron superficially through etching, reducing of moisture, oxidation, photo-oxidation and isomerization of carotenoids (Darvish et al., 2022; Tabibian et al., 2020); therefore, it is essential to define a threshold for acceptability of the color change after treatment. The average values of L^*, a^*, b^*, chroma, and hue of our initial sample were 18.26, 25.85, 16.23, 30.52, and 32.11, respectively. In the treated samples, with the increase of power and time of treatments, L^*, a^*, b^*, and chroma decreased while the hue

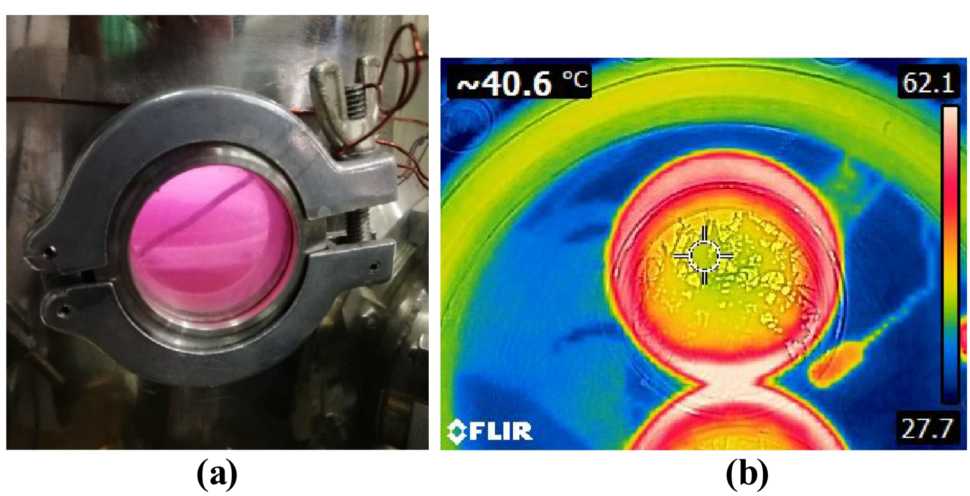

Fig. 5 **a** A saffron sample under plasma treatment. **b** An image taken by the thermal imaging infrared camera of a saffron sample (preliminary test)

Table 8 Correlation coefficients for the design factors and responses

	1	2	3	4	5	6	7	8	9	10	11	12	13	14	15	16	17
1 Run	1																
2 Block	–	–															
3 A:Power	−0.08	–	1														
4 B:Time	−0.03	–	0	1													
5 C:Gas mixture	–	–	–	–	–												
6 Total microorganisms reduced log	−0.09	–	0.79**	0.45**	–	1											
7 *Coliforms* Reduced log	−0.15	–	0.67**	0.43**	–	0.87**	1										
8 Molds and yeasts reduced log	−0.03	–	0.39**	0.60**	–	0.67**	0.72**	1									
9 Crocin	−0.08	–	−0.70**	−0.34*	–	−0.75**	−0.52**	−0.43**	1								
10 Safranal	−0.07	–	0.65**	0.25^{ns}	–	0.52**	0.34*	0.23^{ns}	−0.45**	1							
11 Picrocrocin	0.06	–	−0.81**	−0.27^{ns}	–	−0.71**	−0.59**	−0.45**	0.83**	−0.68**	1						
12 Crocetin	−0.08	–	0.71**	0.24^{ns}	–	0.64**	0.38*	0.28^{ns}	−0.69**	0.81**	−0.73**	1					
13 Coloring strength	−0.27	–	−0.58**	−0.08^{ns}	–	−0.48**	−0.33*	−0.17^{ns}	0.55**	−0.56**	0.60**	−0.57**	1				
14 Aroma	−0.30	–	0.52**	0.37*	–	0.61**	0.51**	0.46**	−0.52**	0.42**	−0.51**	0.54**	0.09^{ns}	1			
15 Bitterness	−0.20	–	−0.60**	−0.21^{ns}	–	−0.50**	−0.48**	−0.35*	0.44**	−0.32*	0.45**	−0.34*	0.80**	0.17^{ns}	1		
16 ΔE_{76}	0.07	–	0.21^{ns}	0.22^{ns}	–	0.44**	0.26^{ns}	0.21^{ns}	−0.47**	0.16^{ns}	−0.23^{ns}	0.49**	−0.09^{ns}	0.51**	0.03^{ns}	1	
17 Desirable function	−0.13	–	0.79**	0.47**	–	0.88**	0.84**	0.70**	−0.56**	0.74**	−0.70**	0.68**	−0.50**	0.57**	−0.49**	0.21^{ns}	1
18 Container temperature	−0.18	–	0.81**	0.38*	–	0.84**	0.81**	0.68*	−0.65**	0.64**	−0.81**	0.65**	−0.45**	0.63**	−0.54**	0.28^{ns}	0.88**
19 Saffron temperature	−0.17	–	0.66**	0.45**	–	0.77**	0.71**	0.72**	−0.58**	0.57**	−0.70**	0.57**	−0.41**	0.55**	−0.57**	0.24^{ns}	0.81**
20 Reduced moisture	0.23	–	0.52**	0.07^{ns}	–	0.43**	0.35*	0.34*	−0.38*	0.37*	−0.43**	0.31*	−0.42**	0.16^{ns}	−0.56**	0.02^{ns}	0.47**
21 Antioxidant activity	−0.11	–	0.34*	−0.13^{ns}	–	0.18^{ns}	0.26^{ns}	0.20^{ns}	−0.11^{ns}	0.03^{ns}	−0.29^{ns}	0.05^{ns}	0.05^{ns}	0.27^{ns}	0.001^{ns}	−0.04^{ns}	0.16^{ns}
22 Total phenol	−0.12	–	0.45**	0.13^{ns}	–	0.41**	0.45**	0.39*	−0.16^{ns}	0.25^{ns}	−0.34*	0.17^{ns}	−0.19^{ns}	0.23^{ns}	−0.36*	−0.21^{ns}	0.50**
23 L^*	0.17	–	−0.62**	−0.23^{ns}	–	−0.52**	−0.33*	−0.21^{ns}	0.47**	−0.64**	0.59**	−0.52**	0.41**	−0.37*	0.34*	−0.02^{ns}	−0.58**
24 a^*	0.18	–	−0.79**	−0.36*	–	−0.74**	−0.52**	−0.40**	0.79**	−0.78**	0.86**	−0.83**	0.61**	−0.61**	0.52**	−0.31*	−0.76**
25 b^*	0.19	–	−0.58**	−0.24^{ns}	–	−0.47**	−0.23^{ns}	−0.15^{ns}	0.58**	−0.74**	0.71**	−0.71**	0.66**	−0.35*	0.47**	−0.02^{ns}	−0.56**
26 Chroma	0.11	–	−0.65**	−0.29^{ns}	–	−0.60**	−0.36*	−0.32*	0.67**	−0.73**	0.76**	−0.75**	0.69**	−0.43**	0.53**	−0.17^{ns}	−0.65**
27 Hue	−0.03	–	0.40**	0.22^{ns}	–	0.52**	0.57**	0.45**	−0.43**	0.07^{ns}	−0.29^{ns}	0.24^{ns}	0.13^{ns}	0.53**	−0.06^{ns}	0.56**	0.37*
28 ΔE_{2000}	0.08	–	0.27^{ns}	0.24^{ns}	–	0.50**	0.39*	0.33*	−0.51**	0.12^{ns}	−0.27^{ns}	0.45**	−0.09^{ns}	0.54**	−0.14^{ns}	0.96**	0.27^{ns}

Table 8 (continued)

	18	19	20	21	22	23	24	25	26	27	28
18 Container temperature	**1**										
19 Saffron temperature	**0.89****	**1**									
20 Reduced moisture	**0.56****	**0.61****	**1**								
21 Antioxidant activity	**0.33***	**0.21**^{ns}	**0.22**^{ns}	**1**							
22 Total phenol	**0.51****	**0.51****	**0.54****	**0.46****	**1**						
23 L*	**−0.57****	**−0.49****	**−0.45****	**−0.18**^{ns}	**−0.38***	**1**					
24 a*	**−0.77****	**−0.66****	**−0.46****	**−0.18**^{ns}	**−0.32***	**0.72****	**1**				
25 b*	**−0.53****	**−0.47****	**−0.34***	**−0.03**^{ns}	**−0.28**^{ns}	**0.65****	**0.88****	**1**			
26 Chroma	**−0.60****	**−0.52****	**−0.36***	**−0.13**^{ns}	**−0.34***	**0.65****	**0.90****	**0.91****	**1**		
27 Hue	**0.48****	**0.38***	**0.24**^{ns}	**0.29**^{ns}	**0.02**^{ns}	**−0.14**^{ns}	**−0.24**^{ns}	**0.23**^{ns}	**0.10**^{ns}	**1**	
28 ΔE_{2000}	**0.35***	**0.29**^{ns}	**0.06**^{ns}	**0.06**^{ns}	**−0.17**^{ns}	**0.04**^{ns}	**−0.30***	**0.06**^{ns}	**−0.13**^{ns}	**0.72****	**1**

ns not significant

*Significant at 5% level; **Significant at 1% level

increased. Tabibian et al. (2020) reported that the L^* and hue decreased in plasma-treated saffron compared to the control compared (Tabibian et al., 2020). They observed an increased value of a^* and no significant changes in b^* and chroma. Darvish et al. (2022) compared the L^*, a^*, and b^* of the plasma-treated saffron samples with the control and reported that treated samples had significantly higher L^* (except for treated samples at 70 W for 10 and 15 min) and higher a^*. Also, they mentioned the lowest b* belonged to the control sample (Darvish et al., 2022).

The ΔE_{76} (color change) of the treated samples ranged from 0.98 through 7.29. It has been noted that ΔE less than 1 or 2 (in different references) is not detectable by the human bare-eyes. Also, $\Delta E^*_{ab} < 5$ is considered a small color change (Mirjalili et al., 2019; Wang et al., 2012). The critical ΔE threshold differs from case to case and is best determined by comparing the values of the ΔE with the results of a panel test. Since there is no reference or standard for the saffron color, we determined the limits by comparing the appearance of the samples with the values of ΔE_{76}, based on Barzegar et al. (2016), by some modifications (Barzegar et al., 2016). These limits are as follows: $\Delta E_{76} < 2$ not detectable, $2 < \Delta E_{76} \leq 4$ detectable yet acceptable; $\Delta E_{76} > 4$ not acceptable. The limit of $\Delta E_{76} > 4$ was applied to set the color goal for optimization. On the other hand, Habekost (2013) indicated that ΔE_{2000} would replace the conventional formula of ΔE_{76} soon because it offers five corrections to the CIElab formula, thus defining the minor color differences the most similar to the human eye perception (Habekost, 2013). Comparing the values of ΔE_{2000} to visual examination revealed that $\Delta E_{2000} \leq 2.5$ is acceptable. Nonetheless, as ΔE_{76} is more common than ΔE_{2000}, it was considered for optimization.

High values of ΔE_{76} were observed in treatments with high power and time. However, we observed no burning of saffron in any of the treated samples, proving that the application of appropriate power and time for plasma treatment decreases neither the visual color quality of the saffron nor its consumer's acceptability (Fig. 6). Hosseini et al. (2018) declared that the saffron color change (ΔE_{76}) after plasma treatment was not visible by the bare eye (Hosseini et al., 2018). Furthermore, ΔE does not determine whether the change made the color better or worse, as some of the treatments made the red color of the saffron stronger and maybe better which needs to be investigated by a panel test. An improvement in the redness of saffron has also been documented after plasma treatment (Tabibian et al., 2020). In addition, some treatments resulted in the more yellow color of the samples, similar to the results of Hertwig et al. (2015b)'s work (Hertwig et al., 2015a, b).

Color change comes after the change of crocin structure as a result of oxidation of its unsaturated bonds and the breaking of glycosidic bonds by oxidizing elements like plasma-free radicals (Tabibian et al., 2020). It was reported that reactive nitrogen species (RNS) in the plasma processed air oxidized carotenoids (Hertwig et al., 2015a, b). Our results indicated that with increasing treatment time and power, crocin and picrocrocin content decreased, but safranal content increased. Similarly, Tabibian et al. (2020) reported that picrocrocin decreased after prolonged exposure to plasma (Tabibian et al., 2020). Sereshti et al. (2018) showed that the amounts of crocin, picrocrocin, and HTCC were high in freshly dried saffron, but safranal content was low. They stated that safranal increased with the decrease in crocin and picrocrocin. It was suggested that picrocrocin could be transformed into safranal by thermal treatment (Sereshti et al., 2018). Our results showed a negative correlation between picrocrocin and safranal which was in agreement with this study. We also observed a positive correlation between crocin and picrocrocin contents. Chaouqi et al. (2018) also declared that samples with higher picrocrocin showed a higher level of safranal after the storage time (Chaouqi et al., 2018).

Crocetin is an important intermediate compound in the biosynthesis pathway of saffron aromatic and coloring agents (Sereshti et al., 2018). Our data revealed that crocetin rises with increasing the treatment time at high powers. Zareena et al. (2001) also reported an increase of crocetin and a decrease of crocin after treating saffron with gamma irradiation (Zareena et al., 2001). We also observed a negative correlation between crocetin and crocin.

Cold plasma technology is an efficient way to deactivate a wide range of foodborne pathogens and non-pathogenic microorganisms (Ekezie et al., 2017). The level of microbial inactivation is dependent on the type of feed gas used to generate the plasma and the treatment time (Segura-Ponce et al., 2018). In literature, some studies concern saffron microbial load and its decontamination (Ghoddusi & Glatz, 2003; Jouki et al., 2011; Khazaei et al., 2011). Cosano et al. (2009) evaluated 33 samples of Iranian saffron and reported that samples contained total aerobic mesophilic bacteria (TAMB) (1 sample), *Enterobacteriaceae* (21 samples), *coliforms* (16 samples), *Clostridium perfringens* (11 samples), *Escherichia coli* (2 samples), molds (2 samples), and yeasts (2 samples). None had more than 10^2 CFU g^{-1} of sulfite-reducing sporulated anaerobic bacteria, *E. coli*, *Bacillus cereus*, and *Clostridium perfringens* (Cosano et al., 2009). Our samples (newly harvested) had 8.05 log CFU g^{-1} of TAMB, 6.71 log CFU g^{-1} of *coliforms*, 4.71 log CFU g^{-1} of molds and yeasts, and 2 log CFU g^{-1} of *E. coli* on average, so our observations were in accordance with the study of Cosano et al. (2009). Different microbial specifications for saffron and other spices emphasize on different contaminating factors with different acceptable limits (Table 13.). Iran has the most comprehensive and strictest microbial standard for saffron. So, it was adopted as a criterion for optimization. On average, samples treated with optimized conditions showed less than 1 log CFU g^{-1} of molds and yeasts. Our result approved the findings of Hosseini et al. (2018), which showed that the application of 60 W oxygen plasma for 15 min completely eradicates mold species. At the optimal conditions, TAMB was reduced by 5.75 log CFU g^{-1} and *coliforms* were eliminated (6.71 log CFU g^{-1}). Akbarian et al. (2019) reported that the maximum decontamination was obtained at 12 min of treatment with a plasma jet (air as the feed gas, 18 kV). They observed 2.69, 2.48, and 1.95 log reduction for the populations of *E. coli*, *E. faecalis*, mold, and yeast, respectively, which shows the lower efficiency of plasma jet compared to low-pressure plasma.

Microbicide effects of the cold plasma are related to the produced reactive species including reactive oxygen and nitrogen species (ROS and RNS) (Mir et al., 2016). Beyrer et al. (2020) achieved 3-log inactivation of *B. coagulans* spores using cold atmospheric plasma and reported that RNS and charged particles were responsible for the spores' coat erosion (Beyrer et al., 2020). The chemistry of plasma is dependent on the feed gas, input voltage and frequency, ambient pressure, and other factors (Ekezie et al., 2017). Different pure gases have been used as the feed gas in plasma sterilization of spices including air (Hertwig et al., 2015a, b), nitrogen (Kim et al., 2014), helium (Kim et al., 2017; Solís-Pacheco et al., 2013), and argon (Hertwig et al., 2015a, b). Also, applying a combination of oxygen or nitrogen with inert gases like helium or argon has been noted (Dorranian et al., 2010; Kim et al., 2014; Salarieh & Dorranian, 2013). Inert gases are added to plasma in order to stabilize the discharge. They produce excited states themselves or excite, ionize, and dissociate other species. It is essential to identify the reactive species produced in a plasma discharge (Whitehead, 2016). Hosseini et al. (2018) found O_2 ions and excited oxygen atoms as the major ROS of O_2 plasma (Hosseini et al., 2018). ROSs play an important role in decontamination because they cause oxidative stress and damage microorganisms' DNA and other biological macromolecules (Pankaj & Keener, 2017).

By comparing the disinfection capacity of the gas mixtures, it was revealed that *X* mixture was better than *Y* mixture in terms of TAMB reduction. Huang et al. (2007) studied the bacterial deactivation effects of a cold argon plasma with oxygen addition and reported that excessive O_2 addition to argon discharge can lead to a decrease in plasma Ar species, which also contribute to bactericidal effects (Huang et al., 2007). This can justify the lower efficacy of *Y* mixture. Although, *Y* mixture showed the highest disinfection capacity for molds and yeasts compared to *X* and *Z* mixtures. Darvish et al. (2022) investigated the cold low-pressure O_2 plasma on saffron, and the highest deactivation levels of the total viable count, *coliforms*, molds, and yeasts were 3.52, 4.62, 2.38, and 4.12 log CFU/g at 110 W for 30 min (Darvish et al., 2022). Our disinfection results of molds and yeasts are similar to this study which shows ROS plays a major role in mold disinfection. Our results showed log reduction of total count (5.75), and *coliforms* (6.71 CFU/g) using the *Y* gas mixture at the level of 76 W for 26 min (optimal conditions) were higher than in this study. These results indicate that other reactive species are major components in bacterial disinfection or synergistically improve the bactericidal power of O_2 plasma. Moreover, a higher level of disinfection can be achieved at lower levels of power and time which reduces the risk of metabolite loss.

UV photons in a low-pressure plasma also play an important role in the inactivation of microorganisms through nucleic acid damage (Moisan et al., 2001). A violet emission from $Ar + O_2$ plasma has been reported in low-pressure cylindrical dc glow discharge plasma (Dorranian & Alizadeh, 2014). Vassallo et al. (2022) found that adding 10–12% N_2 improved the efficacy of low-pressure argon/oxygen RF plasma in the inactivation of *S. aureus* through the synergistic action of UV emission in the range of 200–300 nm and plasma particles. It was also mentioned that this improvement could be due to a higher amount of UV radiation in the $Ar/O_2/N_2$ mixture (Vassallo et al., 2022).

Another mechanism of plasma for microbial destruction is accumulation of excessive charge on the surface of the cells and as a result their disruption. Additionally, cell structures are destructed due to erosion and etching caused by the bombardment of charged particles and energetic ions (Liao et al., 2017). Nishime et al. (2017) investigated the effects of plasma jet on the inactivation of different microorganisms. They observed morphology changes, cell structure modifications, surface damage, and intracellular material leakage in SEM images (Nishime et al., 2017).

Physical changes resulting from the etching phenomenon have been observed in former studies (Hosseini et al., 2018; Tabibian et al., 2020). Our findings were in accordance with them, and our SEM images of saffron also showed cracks and scratches in the surface of the treated sample. Treated pollens showed no surface change that could probably be due to the hard exine layer or was not perceptible at 5000 × magnitude. The porous texture of treated saffron can facilitate the extraction process and develop color in food matrices. Karunanithi et al. (2022) observed that the cold plasma-assisted microwave pretreatment of betel leaf powder improved the extraction yield by 168.18 ± 1.24% (Karunanithi et al., 2022).

Since the samples' temperature was maintained under 50 °C during treatment, the heat may not have been effective in reducing the microbial load. Feroz et al. (2016) evaluated the effect of heat treatment and low-pressure DBD argon plasma treatment on some spices' microbial load, including dried saffron, and they reported that 30 min of 60 °C heat treatment almost did not reduce the bacterial load while increased the fungal load by 1 log (Feroz et al., 2016). Huang et al. (2007) also proved that 5 min of dry heat (125 or 165 °C) carried by the $Ar + O_2$ plasmas had no significant decontamination effects on *E. coli* (Huang et al., 2007). Vassallo et al. (2022) plotted the temperature of samples (the substrate containing the *S. aureus* bacteria) as a function of the treatment time for low-pressure $Ar/O_2/N_2$ RF plasma. Based on the graph, the highest temperature at 100 W was under 50 °C after 5 min, and the curve approached a constant asymptote (Vassallo et al., 2022).

The moisture content of saffron is also an important factor, and its reduction should be considered in any saffron processing because it determines the weight and subsequently the final price. The average moisture of our initial samples was 8.04%. The reduced moisture was increased by increasing the power and time of plasma treatment. It could be a result of both the temperature increase and the microscopic structure change which was evident by SEM images. Our observations were in accordance with the study of Hosseini et al. (2018) and Tabibian et al. (2020). Namjoo et al. (2022) investigated the effect of cold plasma pretreatment before ultrasound-assisted drying of cumin seeds in two exposure times of 15 and 30 s and declared that the cold plasma changed the seed surface morphology and increased the rate of water removal from the interior structure toward the superficial layer (Namjoo et al., 2022).

In the tested range of plasma treatment, antioxidant activity was not considerably changed and only a minor linear decrease was observed by harshening the treatment condition. This reduction was probably due to the reduction of crocin content. Other saffron constituents that are responsible for the antioxidant activity include crocetin, safranal, and phenolic compounds like flavonoids (Tabibian et al., 2020). Hosseini et al. (2018) also stated that cold plasma treatment had no significant effect on antioxidant activity (Hosseini et al., 2018). Phenol content had a weak but significant positive correlation with antioxidant activity ($R^2 = 0.46$) and was decreased by increasing the time and power factors. It has been noted that the plasma ROS could cause the oxidation of phenolic compounds (Chen et al., 2019).

Conclusion

This study showed that the proper processing of saffron with low-pressure radio-frequency cold plasma was able to reduce microorganisms efficiently, without significant loss of metabolites or substantial harm to its appearance. Gas mixture *Y* (65% air/5% O_2/30% Ar) was the best. The time and power of treatment could be set regarding the initial microbial load and the quality of saffron. It was concluded that RF power of 76 W for 26 min with the continuous mode of plasma could decontaminate the saffron to an acceptable level. The color of the treated samples with proper dosage did not show notable change. Investigating the quality of treated saffron after storage and up-scaling of the saffron disinfection with low-pressure RF plasma technology for industrial purposes is recommended.

Appendix

Table 9 Some statistical information on the design responses

	Container temperature	Saffron temperature	Reduced moisture	Antioxidant activity	Total phenol	L^*	a^*	b^*	Chroma	Hue	ΔE_{2000}
Design model	Linear	Reduced Quadratic	Reduced Linear	Reduced Linear	Reduced Quadratic	Reduced Quadratic	Reduced Quadratic	Reduced Quadratic	Reduced Quadratic	Reduced Quadratic	Reduced Quadratic
Model p-value	< 0.0001**	< 0.0001**	0.0002**	0.03*	< 0.0001**	< 0.0001**	< 0.0001**	< 0.0001**	< 0.0001**	< 0.0001**	< 0.0001**
Model *F*-value	48.96	27.03	17.06	5.29	16.90	14.10	54.99	21.67	17.86	10.49	7.48
A- Power *F*-value	154.58	51.98	17.06	5.29	21.00	41.35	194.93	57.40	61.27	18.75	7.08
B-Time *F*-value	34.20	24.10	ni	ni	ni	6.84	42.52	12.04	13.29	4.31	4.74
C- Gas mixture *F*-value	3.53	ni	ni	ni	ni	3.30	ni	4.91	2.78	7.52	0.63
AB *F*-value	ni	ni	ni	ni	ni	ni	7.62	ni	ni	ni	15.07
BC *F*-value	ni	ni	ni	ni	ni	ni	ni	ni	ni	3.09	3.05
A^2 *F*-value	ni	5.01	ni	ni	12.80	ni	22.60	20.84	15.76	3.25	5.37
B^2 *F*-value	ni	ni	Ni	ni	ni	15.72	9.33	33.71	13.34	37.84	25.71
Lack of fit *p*-value	0.051^{ns}	0.34^{ns}	0.08^{ns}	0.51^{ns}	0.92^{ns}	0.34^{ns}	0.78^{ns}	0.31^{ns}	0.81^{ns}	0.54^{ns}	0.24^{ns}
Std. Dev.	4.36	2.21	4.08	0.0003	2.43E-07	0.52	0.89	0.90	1.80	0.84	0.44
R^2	0.84	0.69	0.30	0.12	0.47	0.67	0.89	0.79	0.76	0.72	0.68
Adjusted R^2	0.83	0.66	0.29	0.10	0.44	0.62	0.87	0.76	0.72	0.65	0.59
Predicted R^2	0.78	0.60	0.20	-0.01	0.37	0.53	0.84	0.67	0.65	0.50	0.34
Adequate precision	23.19	14.76	10.31	5.56	10.70	14.33	22.02	13.65	13.05	12.60	11.61

ns not significant, *ni* the term was not included in the model

*significant at 5% level; **Significant at 1% level

Table 10 Some statistical information on the design responses

	Reduced log of total microorganisms	**Reduced log of *coliforms***	**Reduced log of yeasts and molds**	**Crocin**	**Safranal**	**Picrocrocin**	**Crocetin**	**Coloring strength**	**Aroma**	**Bitterness**	**ΔE_{76}**	**Desirable function**
Design model	Reduced quadratic	Reduced quadratic	Reduced quadratic	Reduced quadratic	Reduced quadratic	Reduced quadratic	Reduced quadratic	Reduced quadratic	Reduced quadratic	Linear	Reduced quadratic	Linear
Model *p*-value	< 0.0001**	< 0.0001**	< 0.0001**	< 0.0001**	< 0.0001**	< 0.0001**	< 0.0001**	< 0.0001**	< 0.0001**	< 0.0001**	< 0.0001**	< 0.0001**
Model *F*-value	50.11	29.56	14.48	20.27	20.23	55.42	24.75	12.71	12.83	9.90	7.01	74.31
A- Power *F*-value	241.19	70.41	23.67	87.58	86.76	211.94	88.40	47.78	22.63	31.76	3.74	204.06
B-Time ***F*-value**	76.59	27.33	50.74	19.08	14.44	20.87	7.30	1.16	11.26	3.54	4.12	80.77
C-Gas mixture *F*-value	2.09	ni	0.13	2.53	3.51	ni	ni	7.00	ni	2.14	0.63	6.20
AB *F*-value	ni	ni	ni	5.93	ni	4.60	11.68	5.47	ni	ni	21.60	ni
BC *F*-value	ni	ni	5.57	ni	ni	ni	ni	ni	ni	ni	2.56	ni
AC- *F*-value	4.37	ni	ni	ni	3.83	ni	ni	ni	ni	ni	ni	ni
A^2 *F*-value	ni	10.51	26.94	16.40	9.19	37.43	13.26	15.11	ni	ni	11.31	ni
B^2 *F*-value	20.09	11.58	4.67	6.13	39.41	3.88	4.15	6.93	4.59	ni	13.68	ni
Lack of fit *p*-value	0.30^{ns}	0.72^{ns}	0.67^{ns}	0.41^{ns}	0.24^{ns}	0.57^{ns}	0.14^{ns}	0.07^{ns}	0.13^{ns}	0.12^{ns}	0.17^{ns}	0.73^{ns}
Std. Dev.	0.60	1.11	0.31	11.35	0.08	3.883E-07	0.04	8.88	3.05	6171.81	0.62	190.33
R^2	0.91	0.77	0.78	0.81	0.83	0.89	0.78	0.73	0.51	0.52	0.67	0.89
Adjusted R^2	0.89	0.74	0.73	0.77	0.79	0.87	0.75	0.67	0.47	0.47	0.57	0.88
Predicted R^2	0.85	0.68	0.56	0.69	0.66	0.84	0.66	0.55	0.36	0.34	0.30	0.85
Adequate precision	26.28	14.71	15.52	16.48	16.25	20.59	15.41	14.77	11.40	13.20	11.07	28.31

ns not significant, *ni* the term was not included in the model

**Significant at 1% level

Table 11 Saffron coloring strength, aroma, bitterness and safranal content limits in two specifications

Characteristic	ISO 3632-1 specification (2011)			Azafran de La Mancha PDO specification (2001)	
	Filaments			Bulk Saffron	Packaged Saffron
	Category I	Category II	Category III		
$A^{1\%}_{1\,cm}$ 257 nm	70	55	40	70	70
$A^{1\%}_{1\,cm}$ 330 nm (min–max)	20–50	20–50	20–50	20	20
$A^{1\%}_{1\,cm}$ 440 nm	190	150	100	200	200
Safranal content (% of total volatile components)	–	–	–	65	65

ISO 3632-1 Specification (2011) (ISO, 2011). Azafran de La Mancha PDO specification information is extracted from the study of Cosano et al. (2009) (Cosano et al., 2009)

Table 12 National standard of Iran (No. 259-1) for saffron coloring strength, aroma and bitterness limits

Characteristic	Cut filament	Filaments				Saffron powder			
	Sargol*	Category I	Category II	Category III	Category IV	Sargol	Category I	Category II	Category III
$A^{1\%}_{1\,cm}$ 257 nm	85	80	70	70	70	85	80	70	70
$A^{1\%}_{1\,cm}$ 330 nm (min–max)	20–50	20–50	20–50	20–50	20–50	20–50	20–50	20–50	20–50
$A^{1\%}_{1\,cm}$ 440 nm	220	200	180	150	140	220	200	180	150

Ref: (INSO, 2013)

*Sargol saffron consists of only the red part of the stigma

Table 13 Comparison between some microbiological specifications for saffron and other spices

Contamination		Microbiological specifications				
	National standard of Iran-Saffron (No. 5689)	**National standard of Iran-spices (No. 3677)**	**The Spanish specification—condiments and spices (1984)**	**EU-bacteriological safety of spices (2004)**	**ICMSF-spices, herbs, and dry vegetable seasonings (2005)**	**ICMSF-dry spices and herbs (2011)**
Total aerobic mesophilic bacteria	3×10^5 CFU g^{-1}	5×10^5 CFU g^{-1}	–	–	$<10^6$ CFU g^{-1}	–
Molds and yeasts	10^3 CFU g^{-1}	5×10^3 CFU g^{-1}	–	–	$<10^4$ CFU g^{-1}	–
Escherichia coli	Negative	Negative	<10 CFU g^{-1}	–	$<10^3$ CFU g^{-1}	–
*Enterobacteriaceae**	Negative	–	–	10–10^2 CFU g^{-1}	–	10–10^2 CFU g^{-1}
Coliforms	–	10^3 CFU g^{-1}	–	–	–	–
Sulfite-reducing sporulated anaerobic bacteria (*Clostridia*)**	10^2 CFU g^{-1}	–	$<10^3$ CFU g^{-1}	–	–	–
Clostridium perfringens	–	10^2 CFU g^{-1}	–	10^2 -10^3 CFU g-1	$<10^3$ CFU g^{-1}	–
Salmonella	–	–	0 (in 25 g)	Negative in 25 g	–	Negative
Bacillus cereus	–	10^2 CFU g^{-1}	–	10^3–10^4 CFU g^{-1}	–	–
Heat resistant thermophilic spores	–	–	–	–	–	$<10^2$ CFU g^{-1}
Parasite eggs	–	Negative	–	–	–	–

The Spanish specification and ICMSF- Spices, herbs, and dry vegetable seasonings (2005) information is extracted from the study of Cosano et al. (2009) (Cosano et al., 2009); National standard of Iran—spices (No. 3677) (INSO, 1387)

**Enterobacteriaceae*: This item has been omitted from latest edition of national standard of Iran No. 5689 (INSO, 2018); **sulfite-reducing sporulated anaerobic bacteria (*Clostridia*) are merely counted in vacuum-packed saffron in national standard of Iran number 5689 (INSO, 2018)

Fig. 6 Images of saffron threads in plasma-treated and control samples. In each sample, the label shows the gas mixture type, RF power, and exposure time, respectively. The ratio (%) of air, oxygen, and argon, respectively, in gas mixtures: *X* (50:0:50), *Y* (65:5:30), and *Z* (75:15:10)

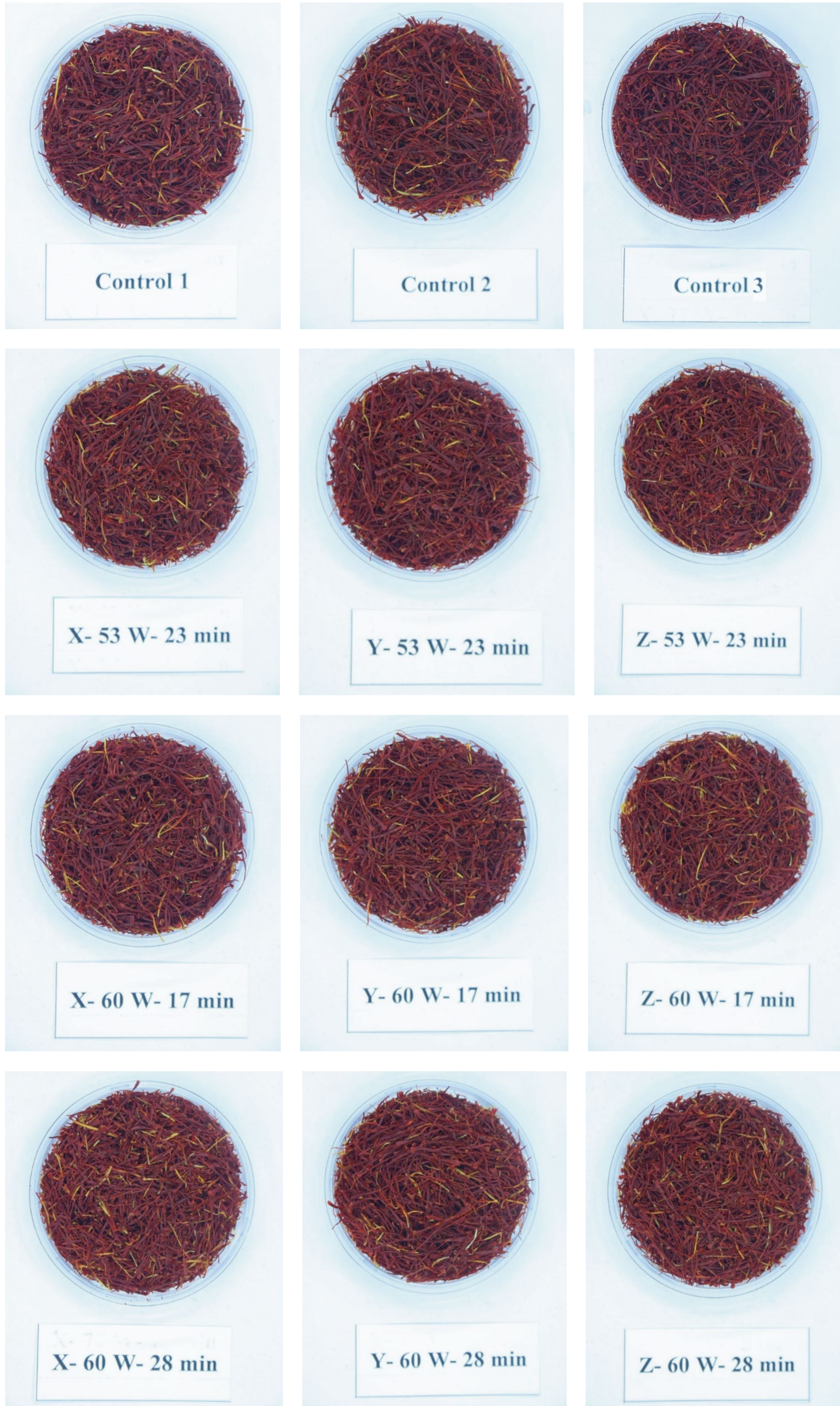

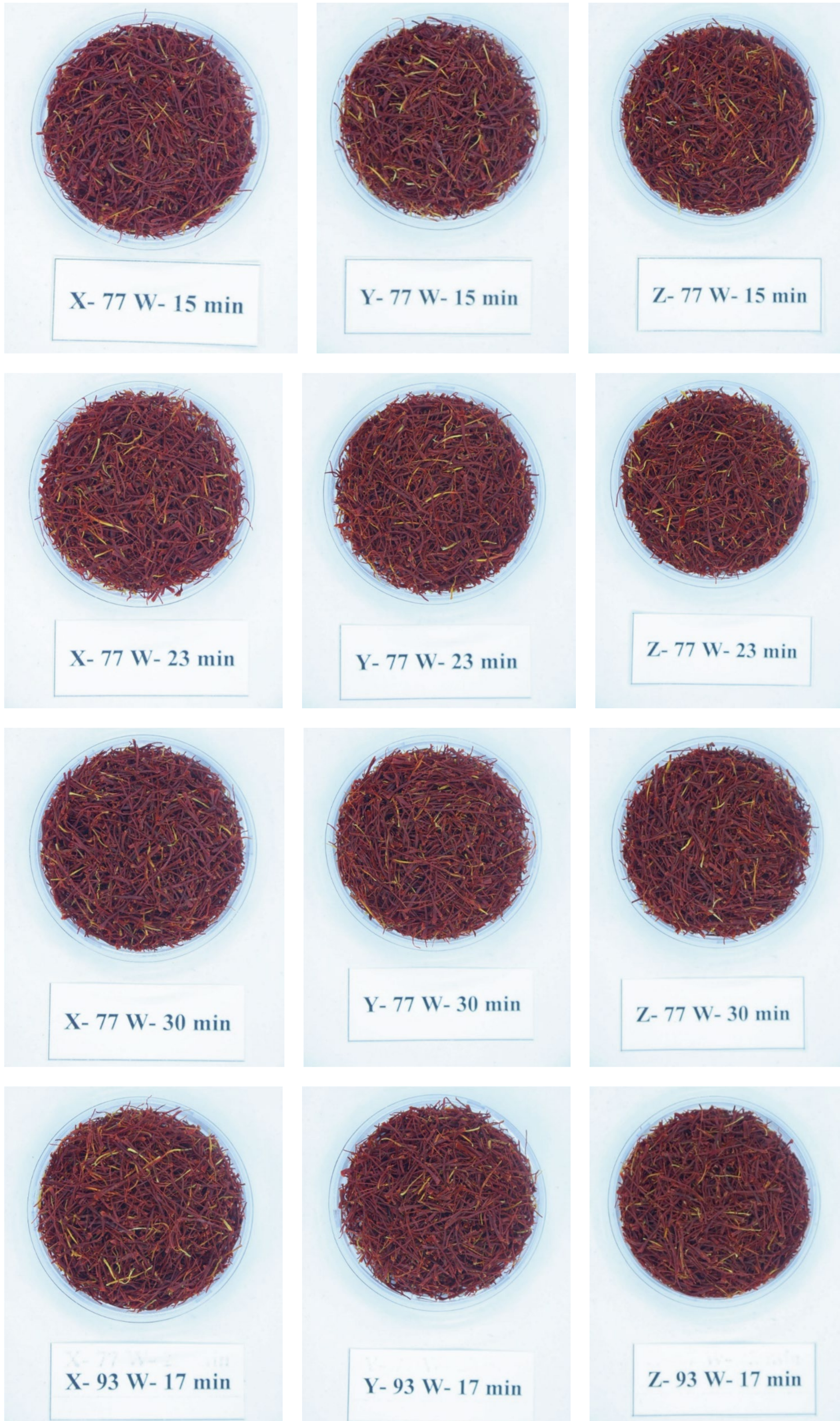

Fig. 6 (continued)

Fig. 6 (continued)

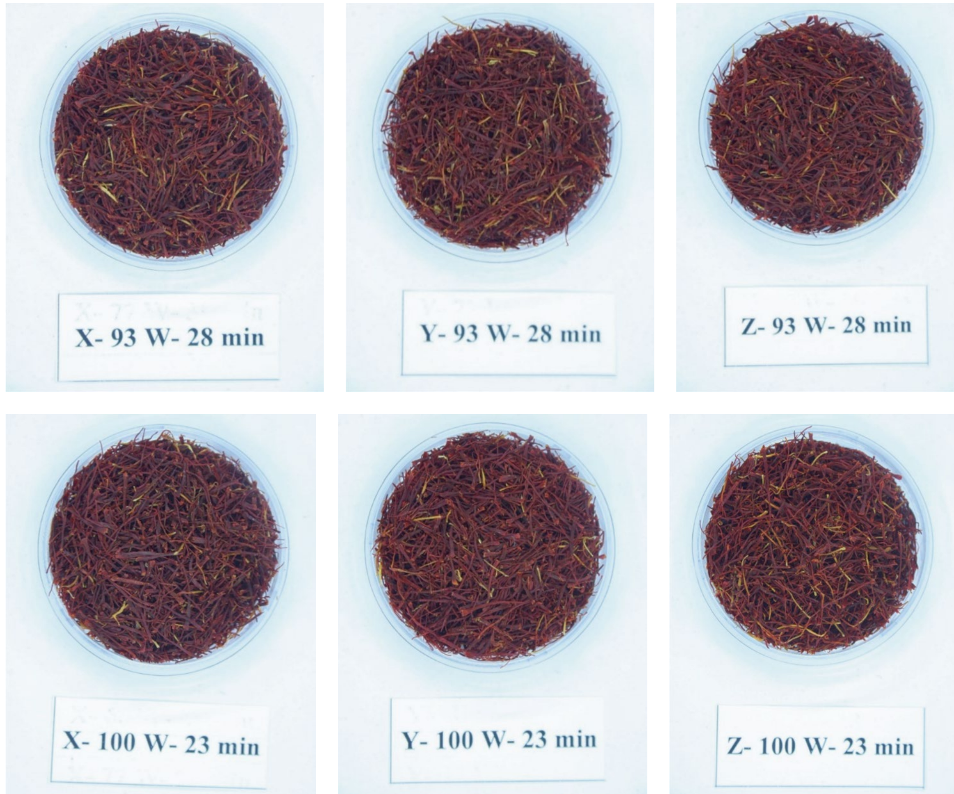

Author Contribution Mahsa Khodabandeh: conceptualization, methodology, investigation, formal analysis, visualization, writing — original draft. Majid Azizi: funding acquisition, project administration, supervision, conceptualization, resources, review and editing. Babak Shokri: resources, review and editing. Masoumeh Bahreini: methodology, resources. Hasan Rezadoost: resources, methodology, review and editing. Mohammad Salehi: investigation, writing — review and editing.

Funding This work was supported by Ferdowsi University of Mashhad (Grant number 48245). This research has also been financially supported by the Saffron Institute, University of Torbat Heydarieh. The grant number was P/99734. Tamim Zarfam Mashreq Zamin Company® (Sarij saffron™ brand) also supported this research under contract number 50856.

Data Availability The data that support the findings of this study are available upon reasonable request from the authors.

Code Availability Not applicable.

Declarations

Ethical Approval This article is an original work and does not involve human participants or animal experimentation.

Consent to Participate and for Publication All the authors declare their consent for participation and publication.

Conflict of Interest The authors declare no competing interests.

References

Aghdaie, S. F. A., Seidi, M., & Riasi, A. (2012). Identifying the barriers to iran's saffron export by using porter's diamond model. *International Journal of Marketing Studies, 4*(5), 129.

Akbarian, M., Shahidi, F., Varidi, M. J., Koocheki, A., & Roshanak, S. (2019). Effect of Cold plasma on microbial and chemical properties of Saffron. *Saffron Agronomy and Technology, 7*(4), 425–439.

Amini, M., Ghoranneviss, M., & Abdijadid, S. (2017). Effect of cold plasma on crocin esters and volatile compounds of saffron. *Food Chemistry, 235*, 290–293.

Azarabadi, N., & Özdemir, F. (2018). Determination of crocin content and volatile components in different qualities of Iranian saffron. *Gıda, 43*(3), 476–489.

Barzegar, M., Seyhoon, M., & Sahari, M. (2016). A study into the effects of gamma-irradiation on bioactivie compounds, color and microbial load of saffron. *Journal of Nuclear Science and Technology (JonSat), 37*(2), 16–25.

Beyrer, M., Smeu, I., Martinet, D., Howling, A., Pina-Pérez, M. C., & Ellert, C. (2020). Cold atmospheric plasma inactivation of microbial spores compared on reference surfaces and powder particles. *Food and Bioprocess Technology, 13*, 827–837.

Cardone, L., Castronuovo, D., Perniola, M., Cicco, N., & Candido, V. (2020). Saffron (*Crocus sativus* L.), the king of spices: an overview. *Scientia Horticulturae*, *272*, 109560.

Castell-Perez, M. E., & Moreira, R. G. (2021). Irradiation and consumers acceptance. *Innovative Food Processing Technologies*, 122–135. https://doi.org/10.1016/B978-0-12-815781-7.00015-9

Chaouqi, S., Moratalla-López, N., Lage, M., Lorenzo, C., Alonso, G. L., & Guedira, T. (2018). Effect of drying and storage process on Moroccan saffron quality. *Food Bioscience, 22*, 146–153.

Chen, C., Liu, C., Jiang, A., Guan, Q., Sun, X., Liu, S., Hao, K., & Hu, W. (2019). The effects of cold plasma-activated water treatment on the microbial growth and antioxidant properties of fresh-cut pears. *Food and Bioprocess Technology, 12*, 1842–1851.

Cosano, I., Pintado, C., Acevedo, O., Novella, J. L., Alonso, G. L., Carmona, M., De La Rosa, C., & Rotger, R. (2009). Microbiological quality of saffron from the main producer countries. *Journal of Food Protection, 72*(10), 2217–2220.

Darvish, H., Ramezan, Y., Khani, M. R., & Kamkari, A. (2022). Effect of low-pressure cold plasma processing on decontamination and quality attributes of Saffron (*Crocus sativus* L.). *Food Science & Nutrition*, *10*(6), 2082–2090.

Das, A., & Sharangi, A. B. (2018). Post harvest technology and value addition of spices. *Indian Spices: The Legacy, Production and Processing of India's Treasured Export*, 249–276.

Dorranian, D., & Alizadeh, M. (2014). Effect of negative oxygen ions on the characteristics of plasma in a cylindrical DC discharge. *Journal of Theoretical and Applied Physics, 8*(2), 1–6.

Dorranian, D., Soudi, M., Jamshidi, M., Sari, A., Nasr, S., & Amini, L. (2010). Sterilization of *Esherichia coli* and the microorganisms of turmeric samples with corona discharge plasma.

Ebadi, M. T., Azizi, M., Sefidkon, F., & Ahmadi, N. (2015). Influence of different drying methods on drying period, essential oil content and composition of Lippia citriodora Kunth. *Journal of Applied Research on Medicinal and Aromatic Plants, 2*(4), 182–187.

Ekezie, F.-G.C., Sun, D.-W., & Cheng, J.-H. (2017). A review on recent advances in cold plasma technology for the food industry: Current applications and future trends. *Trends in Food Science & Technology, 69*, 46–58.

Fallahi, H.-R., Aghhavani-Shajari, M., Sahabi, H., Behdani, M. A., Sayyari-Zohan, M. H., & Vatandoost, S. (2021). Influence of some pre and post-harvest practices on quality of saffron stigmata. *Scientia Horticulturae, 278*, 109846.

Feroz, F., Shimizu, H., Nishioka, T., Mori, M., & Sakagami, Y. (2016). Bacterial and fungal counts of dried and semi-dried foods collected from Dhaka, Bangladesh, and their reduction methods. *Biocontrol Science, 21*(4), 243–251.

Frey, D. D., Engelhardt, F., & Greitzer, E. M. (2003). A role for "one-factor-at-a-time" experimentation in parameter design. *Research in Engineering Design, 14*, 65–74. https://doi.org/10.1007/s00163-002-0026-9

Ghoddusi, H. B., & Glatz, B. (2003). Decontamination of saffron (*Crocus sativus* L.) by electron beam irradiation. *International Symposium on Saffron Biology and Biotechnology, 650*.

Habekost, M. (2013). Which color differencing equation should be used. *International Circular of Graphic Education and Research, 6*, 20–33.

Hertwig, C., Reineke, K., Ehlbeck, J., Erdoğdu, B., Rauh, C., & Schlüter, O. (2015a). Impact of remote plasma treatment on natural microbial load and quality parameters of selected herbs and spices. *Journal of Food Engineering, 167*, 12–17.

Hertwig, C., Reineke, K., Ehlbeck, J., Knorr, D., & Schlüter, O. (2015b). Decontamination of whole black pepper using different cold atmospheric pressure plasma applications. *Food Control, 55*, 221–229.

Hosseini, S. I., Farrokhi, N., Shokri, K., Khani, M. R., & Shokri, B. (2018). Cold low pressure O2 plasma treatment of Crocus sativus: An efficient way to eliminate toxicogenic fungi with minor effect on molecular and cellular properties of saffron. *Food Chemistry, 257*, 310–315.

Hosseinian, S., Maute, C., Rahimi, F., Maute, C., Hamedi, M., & Mirzajani, F. (2020). The influence of ultra-high diluted compounds on the growth and the metabolites of Oriza sativa L. *International Journal of High Dilution Research-ISSN 1982-6206*, *19*(1–2), 39–55.

Huang, C., Yu, Q., Hsieh, F., & h., & Duan, Y. (2007). Bacterial deactivation using a low temperature argon atmospheric plasma brush with oxygen addition. *Plasma Processes and Polymers, 4*(1), 77–87.

INSO. (1387). 3677 Microbiology of spices – specifications. In (1st ed., pp. 1–11): Institute of Standards and Industrial Research of Iran.

INSO. (2013). 259-1 saffron- specification. In (5th ed.): Institute of Standards and Industrial Research of Iran.

INSO. (2018). 5689 Microbiology of saffron – specifications and test methods. In (2nd ed., pp. 1–16): Iranian National Standardization Organization.

ISO. (2008). 21527-2 Microbiology of food and animal feeding stuffs-horizontal method for the enumeration of yeasts and moulds-part 2: colony count technique in products with water activity less than or equal to 0.95. In: International Organization For Standardization, Geneva, Switzerland.

ISO. (2010). 3632–2 spices- saffron- (*Crocus sativus* L.)- part 2: test methods. In: The International Organization for Standardization, Geneva, Switzerland.

ISO. (2011). 3632-1 spices- saffron (*Crocus sativus* L.). Part 1: specifications. In: International Organization For Standardization, Geneva, Switzerland.

ISO. (2013). 4833-1 microbiology of the food chain—horizontal method for the enumeration of microorganisms. Part 2: Colony Count at 30 °C by the Surface Plating Technique. In: The International Organization for Standardization, Geneva, Switzerland.

ISO. (2017). 6887–1 microbiology of the food chain—preparation of test samples, initial suspension and decimal dilutions for microbiological examination. Part 1: General rules for the preparation of the initial suspension and decimal dilutions. In: International Organization for Standardization, Geneva, Switzerland.

Jin, W., Mujumdar, A. S., Zhang, M., & Shi, W. (2018). Novel drying techniques for spices and herbs: A review. *Food Engineering Reviews, 10*(1), 34–45.

Jouki, M., Khazaei, N., Kalbasi, A., Tavakolipour, H., Rajabifar, S., Sedeh, F. M., & Jouki, A. (2011). Study of γ irradiation and storage time on microbial load and chemical quality of persian saffron. *International Journal of Nutrition and Food Engineering, 5*(5), 297–300.

Kabiri, M., Rezadoost, H., & Ghassempour, A. (2017). A comparative quality study of saffron constituents through HPLC and HPTLC methods followed by isolation of crocins and picrocrocin. *LWT, 84*, 1–9.

Karunanithi, S., Guha, P., & Srivastav, P. P. (2022). Cold plasma-assisted microwave pretreatment on essential oil extraction from betel leaves: process optimization and its quality. *Food and Bioprocess Technology*, 1–24.

Khazaei, N., Jouki, M., Kalbasi, A., Tavakolipour, H., Rajabifar, S., Sedeh, F. M., & Jouki, A. (2011). Study of microbial critical points of saffron from farm to factory in Iran. *International Journal of Nutrition and Food Engineering, 5*(5), 293–296.

Khodabandeh, M., Azizi, M., Balandari, A., & Taghizadeh, S. F. (2022). Non-metric multidimensional scaling of barberry (Berberis spp.) genotypes: insights from morphological, nutritional, and biochemical data. *Erwerbs-Obstbau*, 1–14.

Kim, J. E., Lee, D.-U., & Min, S. C. (2014). Microbial decontamination of red pepper powder by cold plasma. *Food Microbiology, 38*, 128–136.

Kim, J. E., Oh, Y. J., Won, M. Y., Lee, K.-S., & Min, S. C. (2017). Microbial decontamination of onion powder using microwave-powered cold plasma treatments. *Food Microbiology, 62*, 112–123.

Liao, X., Liu, D., Xiang, Q., Ahn, J., Chen, S., Ye, X., & Ding, T. (2017). Inactivation mechanisms of non-thermal plasma on microbes: A review. *Food Control, 75*, 83–91.

Maggi, L., Carmona, M., Zalacain, A., Kanakis, C. D., Anastasaki, E., Tarantilis, P. A., Polissiou, M. G., & Alonso, G. L. (2010).

Changes in saffron volatile profile according to its storage time. *Food Research International, 43*(5), 1329–1334.
Mardani, H., Maninang, J., Appiah, K. S., Oikawa, Y., Azizi, M., & Fujii, Y. (2019). Evaluation of biological response of lettuce (Lactuca sativa L.) and weeds to safranal allelochemical of saffron (*Crocus sativus*) by using static exposure method. *Molecules*, *24*(9), 1788.
Mardani, H., Sekine, T., Azizi, M., Mishyna, M., & Fujii, Y. (2015). Identification of safranal as the main allelochemical from saffron (*Crocus sativus*). *Natural product communications*, *10*(5), 1934578X1501000519.
Milani, E. (2020). Assessment and monitoring of saffron microbiological criteria. In *Saffron* (pp. 307–320). Elsevier.
Mir, S. A., Shah, M. A., & Mir, M. M. (2016). Understanding the role of plasma technology in food industry. *Food and Bioprocess Technology, 9*, 734–750.
Mirjalili, F., Luo, M. R., Cui, G., & Morovic, J. (2019). Color-difference formula for evaluating color pairs with no separation: ΔE NS. *JOSA A, 36*(5), 789–799.
Mohamadzadeh Moghadam, M., Taghizadeh, M., Sadrnia, H., & Pourreza, H. R. (2020). Nondestructive classification of saffron using color and textural analysis. *Food Science & Nutrition, 8*(4), 1923–1932.
Moisan, M., Barbeau, J., Moreau, S., Pelletier, J., Tabrizian, M., & L'H, Y. (2001). Low-temperature sterilization using gas plasmas: A review of the experiments and an analysis of the inactivation mechanisms. *International Journal of Pharmaceutics, 226*(1–2), 1–21.
Muhammad, A. I., Xiang, Q., Liao, X., Liu, D., & Ding, T. (2018). Understanding the impact of nonthermal plasma on food constituents and microstructure—a review. *Food and Bioprocess Technology, 11*, 463–486.
Namjoo, M., Moradi, M., Dibagar, N., & Niakousari, M. (2022). Cold plasma pretreatment prior to ultrasound-assisted air drying of cumin seeds. *Food and Bioprocess Technology, 15*(9), 2065–2083.
Nehvi, F., Wani, S., Dar, S., Makhdoomi, M., Allie, B., & Mir, Z. (2006). New emerging trends on production technology of saffron. II International Symposium on Saffron Biology and Technology 739.
Nishime, T., Borges, A., Koga-Ito, C., Machida, M., Hein, L., & Kostov, K. (2017). Non-thermal atmospheric pressure plasma jet applied to inactivation of different microorganisms. *Surface and Coatings Technology, 312*, 19–24.
Nozad, M., Khojastehpour, M., Tabasizadeh, M., Azizi, M., Miraei Ashtiani, S.-H., & Salarikia, A. (2016). Characterization of hot-air drying and infrared drying of spearmint (*Mentha spicata* L.) leaves. *Journal of Food Measurement and Characterization*, *10*(3), 466–473.
Pandey, A., Belwal, T., Sekar, K. C., Bhatt, I. D., & Rawal, R. S. (2018). Optimization of ultrasonic-assisted extraction (UAE) of phenolics and antioxidant compounds from rhizomes of Rheum moorcroftianum using response surface methodology (RSM). *Industrial Crops and Products, 119*, 218–225.
Pankaj, S. K., & Keener, K. M. (2017). Cold plasma: Background, applications and current trends. *Current Opinion in Food Science, 16*, 49–52.
Rajan, A., Boopathy, B., Radhakrishnan, M., Rao, L., Schlüter, O. K., & Tiwari, B. K. (2023). Plasma processing: a sustainable technology in agri-food processing. *Sustainable Food Technology*.
Ranjita Devi, A., Chanchan, M., & Sharangi, A. B. (2018). Why spices are unique? *Indian Spices: The Legacy, Production and Processing of India's Treasured Export*, 31–46.
Rikabad, M. M., Pourakbar, L., Moghaddam, S. S., & Popović-Djordjević, J. (2019). Agrobiological, chemical and antioxidant properties of saffron (*Crocus sativus* L.) exposed to TiO2 nanoparticles and ultraviolet-B stress. *Industrial Crops and Products, 137*, 137–143.
Salarieh, S., & Dorranian, D. (2013). Sterilization of turmeric by atmospheric pressure dielectric barrier discharge plasma. *Plasma Science and Technology, 15*(11), 1122–1126. https://doi.org/10.1088/1009-0630/15/11/09
Salehi, M., Bastani, P., Jamilpanah, L., Madani, A., Mohseni, S. M., & Shokri, B. (2021). Low defect and high electrical conductivity of graphene through plasma graphene healing treatment monitored with in situ optical emission spectroscopy. *Scientific Reports, 11*(1), 20334.
Segura-Ponce, L. A., Reyes, J. E., Troncoso-Contreras, G., & Valenzuela-Tapia, G. (2018). Effect of low-pressure cold plasma (LPCP) on the wettability and the inactivation of Escherichia coli and Listeria innocua on fresh-cut apple (Granny Smith) skin. *Food and Bioprocess Technology, 11*, 1075–1086.
Sereshti, H., Ataolahi, S., Aliakbarzadeh, G., Zarre, S., & Poursorkh, Z. (2018). Evaluation of storage time effect on saffron chemical profile using gas chromatography and spectrophotometry techniques coupled with chemometrics. *Journal of Food Science and Technology, 55*(4), 1350–1359.
Solís-Pacheco, J., Villanueva-Tiburcio, J., Peña-Eguiluz, R., González-Reynoso, O., Cabrera-Díaz, E., González-Álvarez, V., & Aguilar-Uscanga, B. (2013). Effect of plasma energy on the antioxidant activity, total polyphenols and fungal viability in chamomile (*Matricaria chamomilla*) and cinnamon (*Cinnamomum zeylanicum*). *The Journal of Microbiology, Biotechnology and Food Sciences, 2*(5), 2318–2322.
Tabibian, S., Labbafi, M., Askari, G., Rezaeinezhad, A., & Ghomi, H. (2020). Effect of gliding arc discharge plasma pretreatment on drying kinetic, energy consumption and physico-chemical properties of saffron (Crocus sativus L.). *Journal of Food Engineering*, *270*, 109766.
Trademap. (2021). *List of exporters for the selected product in 2021, Product: 091020 Saffron*. https://www.trademap.org/Country_SelProduct.aspx?nvpm=1%7c%7c%7c%7c%7c091020%7c%7c%7c6%7c1%7c1%7c2%7c1%7c1%7c2%7c1%7c1%7c1
Valiasill, R., Azizi, M., & BAHREINI, M., & Arouiee, H. (2013). The investigation of decontamination effects of ozone gas on microbial load and essential oil of several medicinal plants. *Notulae Scientia Biologicae, 5*(1), 34–38.
Vassallo, E., Pedroni, M., Aloisio, M., Silvetti, T., Morandi, S., & Brasca, M. (2022). Synergistic action of reactive plasma particles and UV radiation to inactivate Staphylococcus aureus. *Coatings, 12*(8), 1105.
Wang, H., Cui, G., Luo, M. R., & Xu, H. (2012). Evaluation of colour-difference formulae for different colour-difference magnitudes. *Color Research & Application, 37*(5), 316–325.
Whitehead, J. C. (2016). The chemistry of cold plasma. In *Cold plasma in food and agriculture* (pp. 53–81). Elsevier.
Zareena, A., Variyar, P. S., Gholap, A., & Bongirwar, D. (2001). Chemical investigation of gamma-irradiated saffron (Crocus sativus L.). *Journal of Agricultural and Food Chemistry*, *49*(2), 687–691.